European Journal of Medicinal Chemistry 46 (2011) 3570–3580

Contents lists available at ScienceDirect

European Journal of Medicinal Chemistry

journal homepage: http://www.elsevier.com/locate/ejmech

Original article

Design, synthesis and antiproliferative activities of biarylolefins based on polyhydroxylated and carbohydrate scaffolds

Alexandre Novoa [a], Nadia Pellegrini-Moïse [a], Stéphane Bourg [b], Sylviane Thoret [c], Joëlle Dubois [c], Geneviève Aubert [d], Thierry Cresteil [d], Yves Chapleur [a,*]

[a] UMR 7565 SRSMC, Nancy Université-CNRS, Groupe S.U.C.R.E.S, BP 239, F-54506 Nancy Vandœuvre, France
[b] Fédération de Recherche Physique et Chimie du Vivant, Université d'Orléans, CNRS, FR 2708, Rue Charles Sadron, 45071 Orléans Cedex 2, France
[c] Institut de Chimie des Substances Naturelles, UPR2301 CNRS, Avenue de la Terrasse, F-91198 Gif sur Yvette Cedex, France
[d] Institut de Chimie des Substances Naturelles, Ciblothèque cellulaire, UPR2301 CNRS, Avenue de la terrasse, F-91198 Gif sur Yvette Cedex, France

ARTICLE INFO

Article history:
Received 2 March 2011
Received in revised form
6 May 2011
Accepted 8 May 2011
Available online 13 May 2011

Keywords:
Exo-glycals
Carbohydrates
Biarylolefins
Antiproliferative agents

ABSTRACT

A series of diversely substituted biarylolefins based on carbohydrate and dihydroxyethylene scaffolds were synthesized and evaluated for antiproliferative activity against a panel of human tumor cell lines. Among the thirty-five yet unknown biarylolefins prepared, six displayed potent antiproliferative activities with IC_{50} values in the micromolar and submicromolar range. As a new type of antiproliferative agent, the most potent compound **26** showed an IC_{50} value of 70 nM against SK-OV3 cell line (ovarian cancer). All the synthesized compounds exhibited a poor or modest tubulin polymerization inhibitory activity suggesting another mode of action for these compounds. Molecular docking simulations to the colchicine binding site of tubulin of representative compounds have been used to explain the lack of activity as inhibitors of tubulin polymerization.

1. Introduction

Lignans are naturally occurring compounds found in many plants. These secondary plant metabolites attracted considerable interest due to their anti-inflammatory, immunosuppresive, cardiovascular and antitumor activities. The latter activity has been largely investigated and compounds like podophyllotoxin or its clinically used derivatives. Etoposide, Etopophos, and combretastatins are among the most active representatives of lignans. From a structural point of view, most lignans incorporate two diversely substituted phenyl rings linked through a simple carbon chain as in combretastatins or through more complex, often oxygenated, structures like in podophyllotoxin and isotaxiresinol [1] (Chart 1).

Combretastatin A4 (CA-4) displays a 1,2-diarylethene scaffold bearing two polyoxygenated aromatic rings (Chart 1). It is highly cytotoxic toward several cancer cell lines [2–4] and is a strong inhibitor of tubulin polymerization through binding to the colchicine binding site ($IC_{50} = 1.0$ μM) [5]. The corresponding prodrug water-soluble phosphate (CA4P) is currently in phases II and III clinical trials for the treatment of advanced cancers [6–8]. Many derivatives and analogues have been prepared and evaluated in structure–activity relationships. Among all the synthetic analogues, modifications of ring A, ring B and the double bond have been investigated [9]. CA-4 analogues containing a variety of heterocyclic moieties as surrogates of the olefinic bond have been synthesized and display good cytotoxic activity. The influence of the bridge structure between the two aromatics rings has been largely investigated [10–15]. The replacement of the double bond by a five-membered ring seemed to give the best results, suggesting that the olefinic bond could be modified or expanded. Interestingly, the synthesis and biological evaluations of *cis*-locked vinylogous CA-4 analogues having a cyclopropyl–vinyl or a cyclopropyl–amide bridge have been reported [16].

As a result of SAR studies, the 3,4,5-trimethoxyphenyl A-ring seemed mandatory for antiproliferative activity. The replacement of the isovanillin (B-ring) moiety by a naphthalene ring results in naphtylcombretastatins with cytotoxic activities and inhibition potency of tubulin polymerization comparable to CA-4 [17,18]. Phenstatin, unexpectedly discovered by Petitt's group in the course of a SAR study of combretastatin substituents, was described as a potent cancer cell growth inhibitor with an antitubulin activity similar to that of combretastatin CA-4 ($IC_{50} = 1.2$ μM) (Chart 1) [19].

* Corresponding author. Tel.: +33 383 68 47 43; fax: +33 383 68 47 80.
E-mail address: yves.chapleur@srsmc.uhp-nancy.fr (Y. Chapleur).

0223-5234/$ – see front matter © 2011 Elsevier Masson SAS. All rights reserved.
doi:10.1016/j.ejmech.2011.05.021

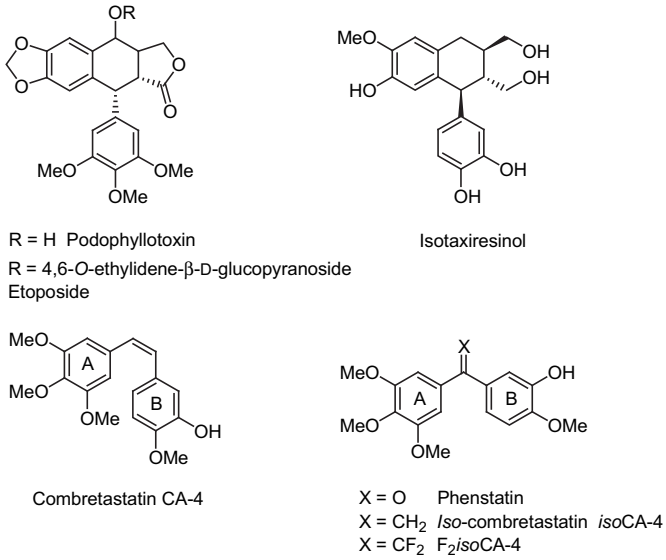

Chart 1. Representative cytotoxic lignans and derivatives.

In phenstatins, the benzophenone structure maintains the appropriate spatial disposition of the two aryl moieties. Several successful structural modifications of phenstatin have been reported [20]. For example, aromatic, heteroaromatic or bicyclic systems have been used to replace the B-ring on the benzophenone scaffold, leading to naphtylphenstatins, indolphenstatins, thienylphenstatins, and others [20–26]. The replacement of the carbonyl group by one-atom or two-atom bridges that maintain the structure of the molecules led to potent derivatives [27–31]. The introduction of an amino group at the C-3 position in B ring of benzophenone strongly enhanced the cytotoxicity [10]. *Iso*-combretastatin A based on a 1,1-diarylethylene scaffold was recently developed and constitutes a novel class of potent antiproliferative agents clearly demonstrating that the carbonyl group is not essential for antitubulin activity [32,33] (Chart 1). Many of the SAR requirements described for combretastatins seemed valuable for phenstatin analogues, in particular the presence of the 3,4,5-trimethoxyphenyl ring and a non-coplanar relationship between the two aromatic rings.

We recently described a facile synthesis of biarylolefins from dibromo-*exo*-glycals using palladium catalyzed cross-coupling reactions [34]. These compounds are closely related to the above-described CA-4 analogues and it seemed interesting to investigate this new class of compounds (Chart 2, type I compounds, 1,1-diaryl-*exo*-glycal) from a biological point of view. The use of carbohydrate scaffold would provide an easy way to modulate the biological activity and the water solubility of the resulting compounds by deprotection of the carbohydrate hydroxyl groups while retaining the cisoid arrangement of the two aromatic rings which seems important for the biological activity of CA4. Moreover, the presence of the sugar ring oxygen would confer some electron-rich character to the double bond and would modify the electronic distribution of the system. This methodology also allows the synthesis of more simple, yet unknown compounds (Chart 2, type II compounds, 1,1-diaryl-2,2-dihydroxymethylethylene) close to isotaxiresinol a recently investigated lignan which proved more active than taxol and doxorubicin against colon adenocarcinoma (Chart 1)[35].

2. Chemistry

Disubstituted *exo*-glycals [36], i.e.; type I compounds, were designed from 1,1-dibromo-D-gulo-hept-1-enitol **1** readily available from the corresponding protected D-gulono-γ-lactone (Scheme 1).

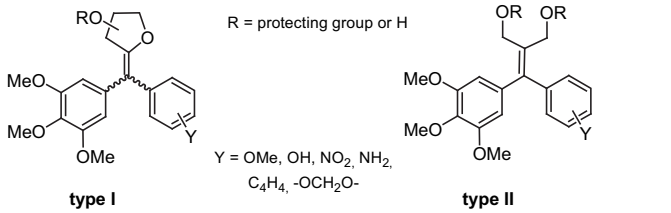

Chart 2. Structures of biarylolefin targets.

Our synthetic strategy involved the sequential introduction of the 3,4,5-trimethoxyphenyl moiety and of a second substituted aromatic or bicyclic aromatic system. The 3,4,5-trimethoxyphenyl ring was first introduced on compound **1** by reaction of 3,4,5-trimethoxyphenyl boronic acid in the presence of tri-(2-furyl) phosphine (TFP) and $PdCl_2(PPh_3)_2$. The monosubstituted (*Z*)-isomer **2** was formed as the major compound obtained in 47% yield using 1.3 eq of boronic acid. The (*E*)-isomer **4** was formed in minute amount (7%) together with the disubstituted compound **3** obtained in 20% yield. A second palladium cross-coupling reaction using $Pd(PPh_3)_4$ was used to introduce the second substituted aromatic moiety. Using this procedure with different boronic acids new disubstituted *exo*-glycals **5**, **7**, **8** and **9** were obtained in good to excellent yields as single stereoisomer. Subsequent removal of the hydroxyl protecting group of **5** by treatment with TBAF afforded the compound **6** bearing the two aromatic moieties of phenstatin (3,4,5-trimethoxyphenyl and isovanillin ring). Catalytic hydrogenation on Pd/C of compound **9** gave the amino derivatives **10** in quantitative yield.

Compound **12**, a geometrical isomer of **6**, was obtained from (*E*)-isomer **4** by cross-coupling reaction with 3-[*tert*-butyldimethylsilyl]oxy]-4-methoxyphenyl]boronic acid [37]. Finally, the diols **13**–**19** were obtained by selective removal of the exocyclic isopropylidene acetal on compounds **3**, **6**–**10** and **12** under acidic conditions.

Simplified analogues, type II compounds (Chart 2), were prepared using the same methodology. The hydroxyl groups of dihydroxyacetone **20** were protected as acetates by treatment with acetic anhydride in pyridine (Scheme 2). Treatment of compound **21** with triphenylphosphine and carbon tetrabromide in dichloromethane at 0 °C led to the yet unknown olefin **22** in 85% yield. Cross-coupling reaction of **22** with 3,4,5-trimethoxyphenyl boronic acid was first investigated using one equivalent of boronic acid in the presence of TFP/$PdCl_2(PPh_3)_2$ in dimethoxyethane. The monosubstituted compound **23** was obtained in less than 20% yield, the starting dibromo compound **22** being recovered. The use of 1.5 eq of 3,4,5-trimethoxyphenyl boronic acid allowed the formation of monosubstituted **23** and disubstituted **24** compounds isolated in 35% and 50% yields respectively. This is likely due to a faster coupling reaction on the monosubstituted derivative **23** as compared to **22**. Commercially available boronic acids and previously synthesized 3-[[*tert*-butyldimethylsilyl]oxy]-4-methoxyphenylboronic acid were used for the preparation of disubstituted compounds **25**–**28**. Removal of *tert*-butyldimethylsilyl group by treatment with TBAF led to the phenolic derivative **26**. Final deprotection of the hydroxyl groups was achieved by treatment by a catalytic amount of sodium methoxide in methanol affording the diols **29**–**32**.

3. Biological evaluation

3.1. Cell culture and cell proliferation assay

The cytotoxicity of some compounds was examined in the National Cancer Institute's Developmental Therapeutics Program

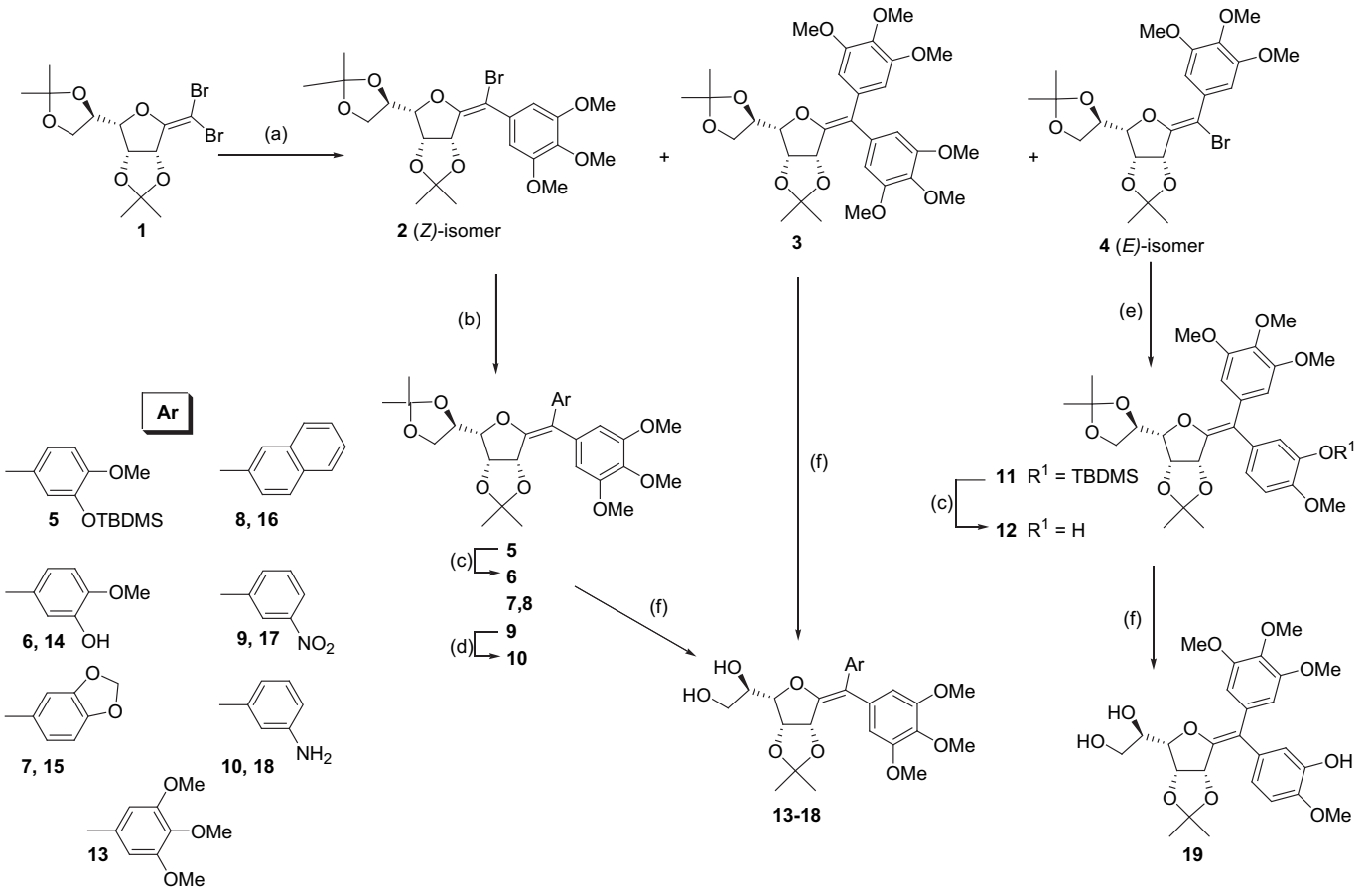

Scheme 1. (a) 3,4,5-Trimethoxyphenylboronic acid (1.3 eq), K_2CO_3 (2 M), trifuryl phosphine, $PdCl_2(PPh_3)_2$, DME, 85 °C, 24 h; (b) $ArB(OH)_2$ (2 eq), K_2CO_3 (2 M), $Pd(PPh_3)_4$, DME, 85 °C, 24 h; (c) Bu_4NF, CH_2Cl_2, 0 °C; (d) H_2, Pd/C, EtOAc; (e) 3-[*tert*-butyldimethylsilyl]oxy]-4-methoxyphenyl] boronic acid (2 eq), K_2CO_3 (2 M), $Pd(PPh_3)_4$, DME, 85°, 24 h; (f) TFA, EtOH, H_2O.

antitumor screening [38]. From our compound library, eleven compounds were selected for pre-screening by the Biological Evaluation Committee and granted NCS codes. These compounds were screened for anti-proliferative activity at a single high dose (10 μM) in the full NCI60 cell panel derived from nine cancer cell types (leukemia, non-small cell lung cancer, colon cancer, CNS cancer, melanoma, ovarian cancer, renal cancer, prostate cancer and breast cancer). A sulforhodamine B (SRB) protein assay was used to estimate cell viability or growth. Results for each compound were reported as the growth percentage of the treated cells when compared to that of the untreated control cells. Selected experimental data and the averaged values of mean graph mid-point (MG-MID) are reported in Supplementary data. Compounds **6**, **8** and **12** which exhibited significant growth inhibition were then selected for re-screening and evaluated against the 60 cell panel at five concentration levels (0.01 μM–100 μM).

Three response parameters (GI_{50}, TGI and LC_{50}) were calculated for each cell line. The GI_{50} value (growth inhibition activity) corresponds to the concentration of compound causing 50% decrease of cell growth while the TGI (total growth inhibition) value (cytostatic activity) is the concentration of the compound resulting in complete growth inhibition. The LC_{50} value (cytotoxic activity) is the concentration of compound leading to 50% loss of initial cells. Table 1 describes the antiproliferative activity using GI_{50} and TGI of selected compounds as mean concentration value (MG-MID) and best activity for each subpanel (I–IX). The GI_{50} and TGI full-panel mean graph mid-point (MG-MID) have also been listed in Table 1. To be concise, only significant results restricted to a few cell lines are listed in Table 2.

Concerning the broad spectrum antitumor activity, the results revealed that the three active compounds **6**, **8** and **12** showed effective growth inhibition GI_{50} (MG-MID) values of 7.41, 5.50 and 10.72 μM respectively, besides cytostatic activity TGI (MG-MID) values of 49.00, 33.90, 55.00 μM respectively (Table 1). The GI_{50} (MG-MID) and TGI (MG-MID) of these three compounds were in the same range of activity against most of the subpanel tumor cell lines. It should be noted that compounds **6** and **12** were found to be slightly less active than **8**. Compound **6** revealed a relative effectiveness on the leukemia, CNS and prostate subpanel (GI_{50} (MG-MID) 4.70, 4.41, 4.20 μM respectively). Regarding cytostatic effect, the highest activity was displayed for CNS subpanel with a TGI (MG-MID) value of 38.3 μM. Excepted against leukemia, compound **8** showed equipotent activity toward growth inhibition with almost all the tested subpanels as revealed by GI_{50} (MG-MID). According to the TGI (MG-MID) values, this compound exhibited the best cytostatic activity against CNS cancer, melanoma and breast cancer subpanels (28.7, 29.3 and 34.5 μM respectively). With GI_{50} (MG-MID) and TGI (MG-MID) values of 10.72 and 55.0 μM, compound **12** appeared as the less powerful compound. Nevertheless, the results showed effective growth inhibition against leukemia, CNS cancer and prostate cancer subpanels (GI_{50} (MG-MID) 8.88, 7.75 and 4.02 μM respectively). Compound **12** was found to have a moderate cytostatic activity, the best effect concerning the melanoma subpanel (TGI (MG-MID) 51.2 μM). These compounds showed

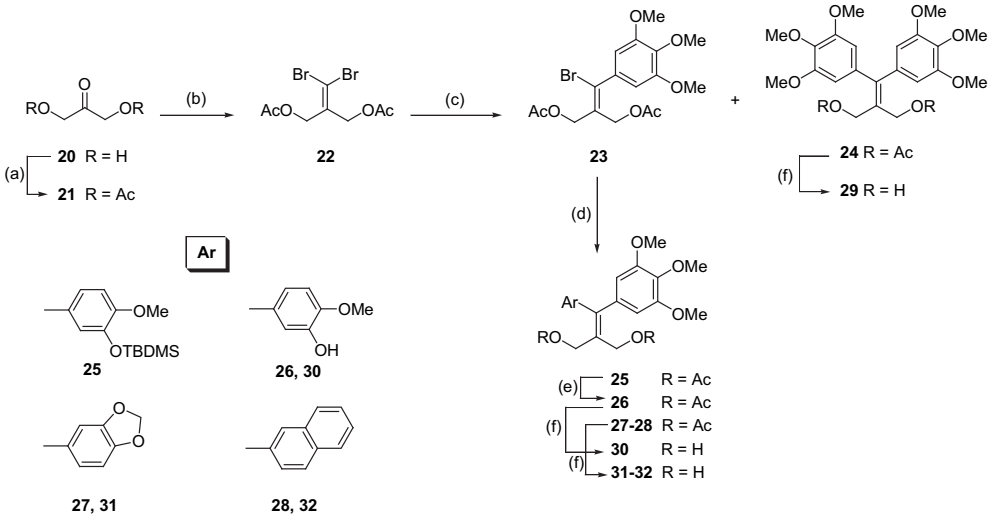

Scheme 2. (a) Ac_2O, DMAP, pyridine; (b) CBr_4, PPh_3, CH_2Cl_2; (c) 3,4,5-trimethoxyphenylboronic acid (1.5 eq), K_2CO_3 (2 M), trifuryl phosphine, $PdCl_2(PPh_3)_2$, DME, 85 °C; (d) $ArB(OH)_2$ (2 eq), K_2CO_3 (2 M), $Pd(PPh_3)_4$, DME, 85 °C, 24 h; (e) Bu_4NF, CH_2Cl_2, 0 °C; (f) Na, MeOH, 0 °C.

a broad spectrum of antitumor activity as well a variable pattern of sensitivity against some individual cell lines (Table 2). With regard to the sensitivity against some selected individual cell lines (Table 2), compounds **6**, **8** and **12** showed high activity against non-small cell lung cancer (NSCLC) NCI-H522 cell line (GI_{50} 2.73, 2.26 and 2.95 and TGI 9.08, 6.54 and 7.54 μM respectively). A noticeable activity against colon cancer HCT-116 cell line (GI_{50} 2.51, TGI 5.70, LC_{50} 20.6 μM) was detected for compound **8** and the analogue **12** also showed a particular effectiveness against colon cancer KM12 cell line (GI_{50} 4.10, TGI 17.8, LC_{50} 72.9 μM). Compound **6** exhibited the highest activity against CNS cancer SNB-75 cell line (GI_{50} 1.80, TGI 6.31 and LC_{50} 53.5 μM). Compound **12** was nearly equipotent against CNS cancer SF-539 cell line with almost the same range of activity (GI_{50} 3.15, TGI 8.75 and LC_{50} 86.0 μM). Melanoma cell lines proved sensitive toward compounds **6**, **8** and **12**. In particular, the highest sensitivity is displayed by SK-MEL-5 cell line with GI_{50}, TGI and LC_{50} values in range of 2.69–4.12, 11.2–15.4 and 47.1–51.4 μM, respectively. The effectiveness of compound **8** against ovarian cancer SK-MEL-2 should be pointed out (GI_{50} 1.53, TGI 4.12 and LC_{50} 24.1 μM). Compounds **6**, **8** and **12** also revealed an obvious sensitivity against ovarian cancer OVCAR-3 cell line with GI_{50} value of 2.38, 2.39 and 4.84 μM values, respectively. The compounds **6, 8** and **12** proved to be moderately sensitive toward renal and breast cancer cell lines, except for renal RXF 393 cell line with growth inhibition concentrations less than 2.6 μM (GI_{50} 2.12, 2.54 and 2.35 μM respectively).

Other compounds not selected in the above-described screening were also evaluated. The cytotoxicity of type II compounds and some 1,1-diaryl-*exo*-glycals (type I) was evaluated on a cell line panel at two concentrations (10^{-5} and 10^{-6} M). Among the ten compounds tested in a preliminary assay (see Supplementary data), those showing some cytotoxicity were further taken for determining their IC_{50} values (Table 3). Three of them, *exo*-glycal derivative **19** and 1,1-diarylethylene derivatives **26** and **32** displayed a potent activity in the micromolar and submicromolar range, IC_{50} values spanning from 70 nM to 6.84 μM. The screening results revealed that these compounds inhibited the growth of all examined tumor cell lines in the same range and that this effect is cell type dependent. The K562 cells line was the most sensitive to **19** and **26**, **32** (IC_{50} 0.45, 0.17, 0.18 μM respectively). It is noteworthy that compound **26** revealed a potent antiproliferative activity on the SK-OV3 cell line (ovarian cancer) (IC_{50} = 70 nM), compounds **32** and **19** being less potent on this cell line (IC_{50} SK-OV3 = 6.51 and 6.84 μM respectively).

3.2. Inhibition of tubulin polymerization

The synthesized derivatives were evaluated for their ability to inhibit tubulin polymerization at a single concentration, phenstatin and deoxypodophyllotoxin being used as positive controls. All the type I and type II compounds (Chart 2) exhibited a modest or poor tubulin polymerization inhibitory activity (see Supplementary data).

Molecular modelling was used to explain this absence of interaction with tubulin. A docking model was constructed starting from the reported X-ray structure of tubulin cocrystallized with a colchicine derivative, *N*-deacetyl-*N*-(2-mercaptoacetyl)colchicine (DAMA-colchicine, PDB entry 1SA0) [39,40]. DAMA-colchicine was first docked to reproduce the co-crystal complex. The docking

Table 1
Mean concentration values (MG-MID) on subpanel and 60 tumor cell lines (μM).

Compounds/NCS code	Subpanel tumor cell lines[a,b]									MG-MID[c]
		I	II	III	IV	V	VI	VII	VIII	IX	
6/753427/1	GI_{50}	4.70/3.22	15.31/2.73	7.88/3.99	4.41/1.80	26.50/1.48	22.38/2.38	17.77/2.12	4.20/3.29	9.36/2.83	7.41
	TGI	87.20/23.30	68.00/9.08	>100/>100	38.3/6.31	68.9/3.70	61.5/5.34	66.90/5.89	66.50/13.3	62.10/7.88	49.00
8/750870/1	GI_{50}	60.09/4.02	4.68/2.26	15.24/2.51	5.47/2.49	3.96/1.53	5.00/2.39	5.24/2.30	5.02/4.33	4.17/3.22	5.50
	TGI	>100/>100	57.80/6.54	74.60/5.70	28.7/7.44	29.30/4.12	49.50/8.02	61.50/4.47	>100/>100	34.50/8.10	33.90
12/750873/1	GI_{50}	8.88/4.82	22.62/2.95	16.72/4.06	7.75/3.15	12.29/2.15	24.47/3.11	18.84/2.35	4.02/3.93	19.78/6.97	10.72
	TGI	81.80/34.0	72.80/7.54	76.60/17.80	58.2/8.75	51.20/5.54	77.70/8.85	71.60/5.07	>100/>100	76.30/50.10	55.00

[a] Subpanel tumor cell lines identification. I, leukemia; II, non-small cell lung cancer; III, colon cancer; IV, CNS cancer; V, melanoma; VI, ovarian cancer; VII, renal cancer; VIII, prostate cancer, IX, breast cancer.
[b] Growth inhibition and cytostatic mean concentration values (MG-MID) on subpanel tumor cell lines/best activity value on subpanel tumor cell lines (μM).
[c] Mean graph mid-point MG-MID: the average sensitivity of all cell lines toward the tested agent.

Table 2
Selected biological activities on NCI-tumor cell lines (μM).

Cell lines		Compounds								
		6			**8**			**12**		
		GI_{50}	TGI	LC_{50}	GI_{50}	TGI	LC_{50}	GI_{50}	TGI	LC_{50}
NSCLC[a]	HOP-62	5.93	25.50	96.80	9.78	31.40	99.80	10.90	34.70	/
	HOP-92	5.45	31.80	/	2.67	13.30	/	4.00	38.30	/
	NCI-H522	2.73	9.08	/	2.26	6.54	/	2.95	7.54	85.60
	HCT-116	4.14	/	/	2.51	5.70	20.6	NT	NT	NT
Colon Cancer	KM12	3.99	/	/	6.00	/	/	4.10	17.80	72.90
	SF-539	2.59	6.63	/	14.30	79.00	/	3.15	8.75	86.00
	SNB-19	4.28	/	/	2.49	6.08	/	5.33	/	/
CNS Cancer	SNB-75	1.80	6.31	53.50	2.89	7.44	/	6.36	/	/
	U251	3.84	48.20	/	3.12	11.80	/	5.00	43.10	/
	LOX IMVI	5.18	/	/	3.39	19.80	/	5.93	22.80	74.10
	MALME-3M	5.46	/	/	2.07	5.59	/	9.96	/	/
Melanoma	MDA-MB-435	1.48	3.70	/	3.61	17.50	/	2.15	5.54	/
	SK-MEL-2	57.90	/	/	1.53	4.12	24.10	3.26	8.43	/
	SK-MEL-5	2.69	11.20	49.30	4.07	15.40	51.40	4.12	15.00	47.10
Ovarian cancer	OVCAR-3	2.38	5.34	22.9	2.39	5.67	21.70	4.84	43.30	/
	NCI/ADR-RES	2.52	6.91	/	4.26	22.30	/	3.11	8.85	/
	786-0	21.20	60.60	/	2.30	4.47	8.60	NT	NT	NT
Renal cancer	RXF 393	2.12	5.89	29.80	2.54	5.99	32.60	2.35	5.07	14.20
Breast cancer	MDA-MB-231/ATCC	4.58	30.70	/	6.28	69.70	/	9.71	50.10	/
	HS 578T	2.83	7.88	/	4.44	53.40	/	6.97	67.90	/

[a] NSCLC = Non-small cell lung cancer; NT: not tested; /: not active, value >100 μM.

mode of the combretastatin A-4 (CA-4), as the lead of numerous compounds interacting with tubulin was examined [16]. The docking mode of phenstatin [19] and phenstatin-like compounds, into the tubulin site was also checked. The best docked poses of CA-4 and phenstatin did nicely superimpose on the DAMA-colchicine X-ray crystal structure (see Supplementary data). Initial conformations of our biaryolefins systems were built and the docking protocol was applied to compound **30**. The best poses obtained for phenstatin, *iso*CA-4, F_2*iso*CA-4 and **30** showed a common binding mode corresponding to that previously determined. Docking experiments showed that **30** could assume the same binding mode as CA-4 or phenstatin.

The 3D energy minimized conformation of **6** was superimposed by hand on docked phenstatin into the colchicine binding site of tubulin (Fig. 1, red surface). Protein flexibility is supposed to allow such a conformation. Docking of compound **6** was next carried out. As seen from Fig. 1, poses fill in the open cavity but in different orientations. Moreover they are disordered and do not bind in a coherent mode showing two, one or no hydrogen bond(s) with Cys β 241 and or Thr β 353. Compound **6** poses are essentially oriented toward the solvent, losing the required interactions of tubulin inhibitors in the binding site.

Table 3
Inhibition of cancer cell proliferation (IC_{50}, μM).

Cells lines		Compounds		
		19	**26**	**32**
Colon cancer	HCT15	0.63	0.68	0.39
Breast cancer	MDA231	0.61	1.03	0.81
Prostate cancer	PC3	0.69	0.27	0.76
Glioblastoma	SF268	1.10	0.97	1.25
Ovarian cancer	SK-OV3	6.51	0.07	6.84
	OVCAR8	2.97	1.90	4.47
Lymphoblastoma	HL60	0.82	0.68	0.78
	HL60R	1.49	2.72	1.68
	K562	0.45	0.18	0.17

4. Discussion

The screening results revealed that four 1,1-diaryl-*exo*-glycals (type I compounds) and two derivatives belonging to type II showed a significant antiproliferative effect in the micromolar and submicromolar range (Chart 3). From these results it appears that a set of three compounds **6**, **8** and **12** exhibit growth inhibition with GI_{50} in the 7–11 μM range associated with cytostatic activities in the 34–55 μM range. All three compounds are active against renal cancer (RXF-393). It is to note that compounds **6** and **12** are geometric isomers which behave similarly on the RXF-393 cell line although **12** is less active than **6** against other cell lines. It is worth to mention that these most active compounds have the same aromatic substituents than CA-4 or phenstatin. Moreover compound **8** embodies a napthalene ring which has been shown to enhance the activity of combretastatin [17,18] or phenstatin analogues [23]. Three other compounds **19**, **26** and **32** revealed interesting growth inhibition properties on all examined tumor cell lines in the same range with IC_{50} below 1 μM but this effect is cell type dependent. Examination of Chart 3 clearly shows that the highest powerful inhibition of cell proliferation was obtained with yet unknown 1,1-diarylethylene derivatives **26** and **32** (type II compounds), the 1,1-diaryl-*exo*-glycal **19** being slightly less active. However, the latter is the most active compound of the type I class of compounds. This could be a consequence of the presence of a diol function instead of the more bulky 5,6-dioxolane ring present in compounds **6**, **8** and **12**. It should also be noted that the dihydroxylated compound **30**, is much less active than its acetylated derivative **26** whereas **32** is more active than its acetylated derivative **28** suggesting that, in these compounds, the hydroxyl groups do not play a key role. Compounds **26** and **32** revealed potent activity toward SK-OV3 and K563 cell lines. Finally the most active compound was the biarylolefin **26** with an $IC_{50} = 70$ nM against SK-OV3, ovarian cancer.

An important result is the almost complete lack of inhibition of tubulin polymerization of all compounds of this study. Thus the observed inhibition of cell proliferation is not due to interaction

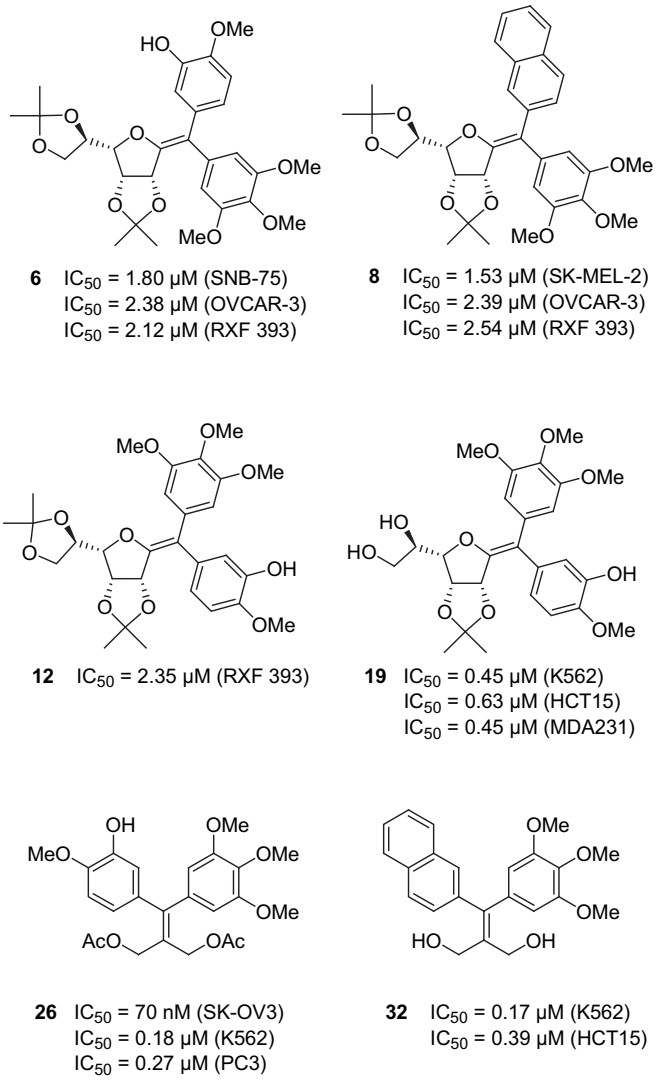

Chart 3. Structures and selected activities for the most potent compounds.

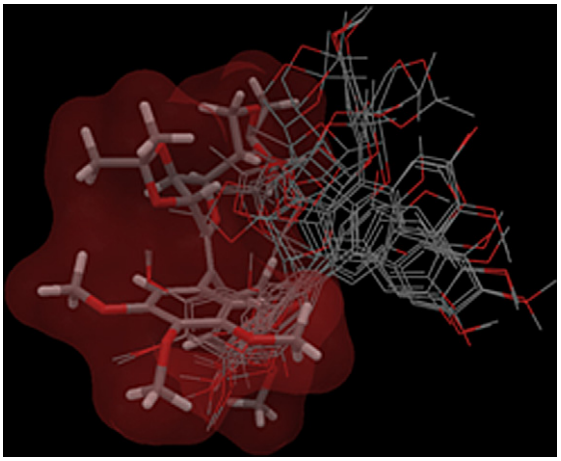

Fig. 1. The ten best docked poses of compound **6** superimposed to the "by hand" docked conformation of **6** (red surface). Poses are represented without hydrogen atoms for clarity. (For interpretation of the references to colour in this figure legend, the reader is referred to the web version of this article.)

with tubulin. However, a COMPARE analysis [41,42] which measures the correlation between two compounds with respect to their differential antiproliferative activity has been carried out on the most active compounds but failed to provide any significant match to a known compound and any associated mechanism of action.

Molecular modelling studies revealed that interaction of our 1,1-diarylolefins like **30** with the colchicine binding site to tubulin is possible. As **30** is not a significant inhibitor of tubulin, this suggests that the presence of the two hydroxyl groups may induce other interactions (for example hydrogen bonding) not taken into account in the docking model, which do not allow a correct arrangement of **30** in the colchicine site of tubulin. The binding model of **30** revealed the presence of an open cavity above the two hydroxyl groups in agreement with previous reports [16,43]. It should be noted that active *iso*-combretastatin analogues mostly include on the double bond a rather flat moiety which could be accommodated in this putative open space. In our case, the sugar moiety of compound like **6**, is too voluminous for this open space likely because of the presence of one or two dioxolane rings on the sugar ring. This precludes our compounds to adopt the correct orientation of the aromatic rings in the colchicine binding site. Thus, the introduction of too bulky susbtituents on *iso*-combretastatin double bond clearly abolishes the antitubulin activity and the mode of action of our compounds should be different. A good example of changing the mode of action by introduction of a rather bulky substituent on a tubulin polymerization inhibitor can be found in the podophyllotoxin series. Thus, podophyllotoxin is a tubulin polymerization inhibitor while etoposide, its glycosylated is a topoisomerase II inhibitor [44–46].

5. Conclusion

We have discovered a new class of antiproliferative agents based on a biarylolefin motif. Two types of derivatives have been designed on carbohydrate and dihydroxymethylethylene scaffolds (type I and II compounds) and were synthesized by a straightforward approach using sequential palladium cross-coupling reaction. This flexible strategy allows the sequential addition of different aromatic rings at a late stage of the synthesis in contrast to phenstatin analogue syntheses, which start from benzophenone derivatives. Thirty-five new compounds have been prepared among which six displayed a broad spectrum of antitumor activity in the micromolar or submicromolar range. A variable pattern of sensitivity against some individual cell lines was observed and the most potent compound **26** revealed a high activity toward an ovarian cancer cell line ($IC_{50} = 70$ nM, SK-OV3). None of the synthesized compounds exhibited tubulin polymerization inhibitory activity, a tentative explanation suggested by molecular modelling could be a steric hindrance induced by the double bond substituents or by other interactions due to the presence of free hydroxyl or ester groups on these compounds. These results suggested that the cell proliferation inhibition activity of our compounds could be attributed to another mechanism of action. More biological experiments are underway to determine a possible mechanism, which would give some information on how to improve the efficiency of our leads by chemical structure modulation.

6. Experimental section

6.1. Chemistry

6.1.1. Material and methods

All reagents were commercially available and were used without further purification unless otherwise indicated. DME was

stored on activated molecular sieves (4 Å) and dichloromethane was dried by distillation from calcium hydride prior to use. TLC analyses were performed using standard procedures on Kieselgel 60 F254 plates (Merck). Compounds were visualized using UV light (254 nm) and 30% methanolic H_2SO_4/heat as developing agent. Column chromatography was performed on silica gel SI 60 (63–200 μm) (Merck). FTIR spectra were recorded on a Perkin–Elmer spectrum 1000 on film windows. Melting points were determined in capillary tubes and are uncorrected. Optical rotations were measured on a Perkin–Elmer 141 polarimeter. ^{1}H and ^{13}C NMR spectra were recorded on a Bruker spectrometer DPX250 (250 MHz and 62.9 MHz, respectively) and DRX400 (400 MHz and 100.6 MHz, respectively). For complete assignment of ^{1}H and ^{13}C signals, two-dimensional ^{1}H, ^{1}H COSY and ^{1}H, ^{13}C correlation spectra were recorded. Chemical shifts (δ) are given in ppm relative to the solvent residual peak. The following abbreviations are used for multiplicity of NMR signals: s = singlet, d = doublet, t = triplet, q = quadruplet, m = multiplet, br = broad signal. For the sake of simplicity, nomenclature is inspired from that of carbohydrates. HRMS spectra were recorded on a Bruker MicroTOFQ apparatus. Microwave syntheses were performed in a mono-mode oven, the temperature being controlled with a standard external IR-sensor. Analytical high-performance liquid chromatography (HPLC) was performed using a Spectra P1000XR apparatus with an Interchim UP50DB-25QS C18 reverse phase 250 mm × 4.6 mm column. Samples were detected using an absorbance detector UV150 (wavelength of 254 nm). The flow rate of the mobile phase (water/acetonitrile 3/7) was of 1 mL/min. The purity of the tested compounds was determined by HPLC and unless otherwise stated, the purity level was ≥95%. Details of the synthesis and characterizations of intermediate compounds are given in the Supplementary data.

6.1.2. General procedure for first cross-coupling reaction

In a dry round-bottomed flask equipped with a condenser flushed with argon, 5 mL of dry DME, dibromo-*exo*-glycal **1** (150 mg, 0.362 mmol, 1 eq), 3,4,5-trimethoxyphenylboronic acid (100 mg, 0.47 mmol, 1.3 eq), 2 M K_2CO_3 aqueous solution (2.6 eq) were stirred for 10 min. Tris-(2-furyl)phosphine (26 mg, 0.109 mmol, 0.3 eq) and $PdCl_2(PPh_3)_2$ (13 mg, 0.018 mmol, 0.05 eq) were added as solids. The reaction mixture was stirred and heated at 85 °C during 24 h. The reaction was then allowed to cool to room temperature and was concentrated under reduced pressure. The residue was diluted with ethyl acetate (50 mL) and washed with NH_4Cl (2 × 5 mL). The dried organic layer was evaporated under reduced pressure and the residue was purified by chromatography (*n*-hexane/EtOAc).

*6.1.2.1. (Z)-2,5-Anhydro-1-bromo-1-(3,4,5-trimethoxyphenyl)-1-deoxy-3,4:6,7-di-O-isopropylidene-D-gulo-hept-1-enitol (**2**).* Yield: 47% as a pale yellow solid; R_f = 0.33 (Hexane/EtOAc 7/3); $[\alpha]_D^{20} = -228°$ (c = 0.95, $CHCl_3$); IR (film) ν 2987, 2933, 1655, 1580, 1504 cm^{-1}; ^{1}H NMR ($CDCl_3$, 400 MHz) δ 1.33 (s, 3H, C(CH_3)$_2$), 1.44 (s, 3H, C(CH_3)$_2$), 1.51 (s, 3H, C(CH_3)$_2$), 1.55 (s, 3H, C(CH_3)$_2$), 3.77 (dd, 1H, *H*-7, *J* = 8.5 Hz, *J* = 7.0 Hz), 3.88 (s, 9H, 3 OCH_3), 4.16 (dd, 1H, *H*-5, *J* = 8.0 Hz, *J* = 5.0 Hz), 4.26 (dd, 1H, *H*-7′, *J* = 8.5 Hz, *J* = 7.0 Hz), 4.51 (dt, 1H, *H*-6, *J* = 8.0 Hz, *J* = 7.0 Hz), 4.82 (dd, 1H, *H*-4, *J* = 6.0 Hz, *J* = 5.0 Hz), 4.99 (d, 1H, *H*-3, *J* = 6.0 Hz), 6.93 (s, 2H, *H*–Ar); ^{13}C NMR ($CDCl_3$, 62.9 MHz) δ 25.1 (C(CH_3)$_2$), 25.3 (C(CH_3)$_2$), 26.2 (C(CH_3)$_2$), 26.8 (C(CH_3)$_2$), 56.0 (2 OCH_3), 60.9 (OCH_3), 65.9 (*C*-7), 75.8 (*C*-6), 79.0 (*C*-4), 79.4 (*C*-3), 85.4 (*C*-5), 101.0 (*C*-1), 107.0 (2 *C*–Ar), 110.0 (*C*(CH_3)$_2$), 113.1 (*C*(CH_3)$_2$), 132.4 (*C*–Ar), 137.9 (*C*–Ar), 152.1 (*C*-2), 152.5 (2 *C*–Ar); HRMS (ESI) calculated for $C_{22}H_{29}BrNaO_8$: 523.0938, $[M + Na]^+$ found 523.0933.

*6.1.2.2. 2,5-Anhydro-1.1-di(3,4,5-trimethoxyphenyl)-1-deoxy-3,4:6,7-di-O-isopropylidene-D-gulo-hept-1-enitol (**3**).* Yield: 20% as a pale yellow solid; R_f = 0.20 (Hexane/EtOAc 7/3); $[\alpha]_D^{20} = -225°$ (c = 0.93, $CHCl_3$); IR (film) ν 2987, 2933, 1645, 1580, 1508 (OMe) cm^{-1}; ^{1}H NMR ($CDCl_3$, 250 MHz) δ 1.28 (s, 3H, C(CH_3)$_2$), 1.35 (s, 3H, C(CH_3)$_2$), 1.41 (s, 3H, C(CH_3)$_2$), 1.48 (s, 3H, C(CH_3)$_2$), 3.75 (s, 6H, 2 OCH_3), 3.76 (m, 1H, *H*-7), 3.79 (s, 6H, 2 OCH_3), 3.83 (s, 3H, OCH_3), 3.87 (s, 3H, OCH_3), 4.03 (dd, 1H, *H*-5, *J* = 8.5 Hz, *J* = 4.5 Hz), 4.22 (dd, 1H, *H*-7′, *J* = 8.5 Hz, *J* = 7.0 Hz), 4.47 (dt, 1H, *H*-6, *J* = 8.5 Hz, *J* = 7.0 Hz), 4.70 (dd, 1H, *H*-4, *J* = 6.0 Hz, *J* = 4.5 Hz), 4.94 (d, 1H, *H*-3, *J* = 6.0 Hz), 6.63 (s, 2H, *H*–Ar), 6.72 (s, 2H, *H*–Ar); ^{13}C NMR ($CDCl_3$, 62.9 MHz) δ 25.1 (C(CH_3)$_2$), 25.1 (C(CH_3)$_2$), 26.3 (C(CH_3)$_2$), 26.8 (C(CH_3)$_2$), 55.9 (2 OCH_3), 56.0 (2 OCH_3), 60.8 (OCH_3), 60.8 (OCH_3), 65.8 (*C*-7), 75.5 (*C*-6), 78.3 (*C*-4), 80.5 (*C*-3), 85.2 (*C*-5), 107.3 (2 *C*–Ar), 108.2 (2 *C*–Ar), 109.7 (*C*(CH_3)$_2$), 112.6 (*C*(CH_3)$_2$), 120.5 (*C*-1), 133.8 (*C*–Ar), 134.2 (*C*–Ar), 136.9 (*C*–Ar), 137.0 (*C*–Ar), 150.6 (*C*-2), 152.4 (2 *C*–Ar), 152.5 (2 *C*–Ar); HRMS (ESI) calculated for $C_{31}H_{40}NaO_{11}$: 611.2463, $[M + Na]^+$ found 611.2471.

*6.1.2.3. (E)-2,5-Anhydro-1-bromo-1-(3,4,5-trimethoxyphenyl)-1-deoxy-3,4:6,7-di-O-isopropylidene-D-gulo-hept-1-enitol (**4**).* Yield: 7% as a pale yellow solid; R_f = 0.44 (Hexane/EtOAc 7/3); ^{1}H NMR ($CDCl_3$, 250 MHz) δ 1.36 (s, 3H, C(CH_3)$_2$), 1.42 (s, 3H, C(CH_3)$_2$), 1.43 (s, 3H, C(CH_3)$_2$), 1.50 (s, 3H, C(CH_3)$_2$), 3.79 (dd, 1H, *H*-7, *J* = 8.5 Hz, *J* = 6.5 Hz), 3.86 (s, 3H, OCH_3), 3.88 (s, 6H, 2 OCH_3), 4.18 (dd, 1H, *H*-5, *J* = 8.5 Hz, *J* = 4.0 Hz), 4.23 (dd, 1H, *H*-7′, *J* = 8.5 Hz, *J* = 6.5 Hz), 4.49 (dt, 1H, *H*-6, *J* = 8.5 Hz, *J* = 6.5 Hz), 4.74 (dd, 1H, *H*-4, *J* = 6.0 Hz, *J* = 4.0 Hz), 5.51 (d, 1H, *H*-3, *J* = 6.0 Hz), 7.16 (s, 2H, *H*–Ar); ^{13}C NMR ($CDCl_3$, 62.9 MHz) δ 25.2 (C(CH_3)$_2$), 25.7 (C(CH_3)$_2$), 26.5 (C(CH_3)$_2$), 26.8 (C(CH_3)$_2$), 55.9 (2 OCH_3), 60.8 (OCH_3), 65.8 (*C*-7), 75.4 (*C*-6), 78.0 (*C*-4), 82.9 (*C*-3), 86.1 (*C*-5), 102.1 (*C*-1), 106.3 (2 *C*–Ar), 109.8 (*C*(CH_3)$_2$), 113.6 (*C*(CH_3)$_2$), 131.1 (*C*–Ar), 137.4 (*C*–Ar), 152.0 (*C*-2), 152.4 (2 *C*–Ar); HRMS (ESI) calculated for $C_{22}H_{29}BrNaO_8$: 523.0936, $[M + Na]^+$ found 523.0938.

6.1.3. General procedure for second cross-coupling reaction

In a dry round-bottomed flask equipped with a condenser flushed with argon, 5 mL of dry DME, bromo-*exo*-glycals **2** or **4** (0.362 mmol), boronic acid (2 eq), 2 M K_2CO_3 aqueous solution (4 eq) were stirred for 10 min. Solid $Pd(PPh_3)_4$ (20 mg, 0.018 mmol, 0.05 eq) was then added. The reaction mixture was stirred and heated at 85 °C during 24 h. The reaction was then allowed to cool to room temperature and was evaporated to dryness under reduced pressure. The residue was diluted with ethyl acetate (50 mL) and washed with NH_4Cl (2 × 5 mL). The dried organic layer was evaporated under reduced pressure and the residue was purified by chromatography (*n*-hexane/EtOAc).

*6.1.3.1. (Z)-2,5-Anhydro-1-(3-tertbutyldimethylsilyloxy-4-methoxyphenyl)-1-(3,4,5-trimethoxyphenyl)-1-deoxy-3,4:6,7-di-O-isopropylidene-D-gulo-hept-1-enitol (**5**).* Yield: 70% as a pale yellow solid; R_f = 0.36 (Hexane/EtOAc 7/3); $[\alpha]_D^{20} = -184°$ (c = 0.57, $CHCl_3$); IR (film) ν 2987, 2954, 2927, 2851, 1645, 1583, 1508 cm^{-1}; ^{1}H NMR ($CDCl_3$, 400 MHz) δ 0.16 (s, 3H, Si(CH_3)$_2$), 0.17 (s, 3H, Si(CH_3)$_2$), 0.99 (s, 9H, SiC(CH_3)$_3$), 1.29 (s, 3H, C(CH_3)$_2$), 1.40 (s, 3H, C(CH_3)$_2$), 1.49 (s, 3H, C(CH_3)$_2$), 1.51 (s, 3H, C(CH_3)$_2$), 3.78 (m, 1H, H-7), 3.80 (s, 9H, 3 OCH_3), 3.89 (s, 3H, OCH_3), 4.12 (dd, 1H, *H*-5, *J* = 8.5 Hz, *J* = 5.0 Hz), 4.26 (dd, 1H, *H*-7′, *J* = 8.5 Hz, *J* = 7.0 Hz), 4.47 (dt, 1H, *H*-6, *J* = 8.5 Hz, *J* = 7.0 Hz), 4.71 (dd, 1H, *H*-4, *J* = 6.0 Hz, *J* = 5.0 Hz), 4.96 (d, 1H, *H*-3, *J* = 6.0 Hz), 6.60 (s, 2H, *H*–Ar), 6.77 (d, 1H, *H*–Ar, *J* = 8.5 Hz), 6.90 (dd, 1H, *H*–Ar, *J* = 8.5 Hz, *J* = 2.0 Hz), 7.09 (d, 1H, *H*–Ar, *J* = 2.0 Hz); ^{13}C NMR ($CDCl_3$, 62.9 MHz) δ −4.6 (Si(CH_3)$_2$), −4.5 (Si(CH_3)$_2$), 18.4 (SiC(CH_3)$_3$), 25.2 (C(CH_3)$_2$), 25.3 (C(CH_3)$_2$), 25.8 (3 SiC(CH_3)$_3$), 26.2 (C(CH_3)$_2$), 26.9 (C(CH_3)$_2$), 55.5 (OCH_3), 55.9 (2 OCH_3), 60.9 (OCH_3),

65.9 (*C*-7), 76.1 (*C*-6), 78.3 (*C*-4), 80.4 (*C*-3), 85.4 (*C*-5), 108.1 (2 *C*–Ar), 109.7 (*C*(CH_3)$_2$), 111.5 (*C*–Ar), 112.4 (*C*(CH_3)$_2$), 119.6 (*C*-1), 122.3 (*C*–Ar), 123.2 (*C*–Ar), 131.4 (*C*–Ar), 135.1 (*C*–Ar), 136.8 (*C*–Ar), 144.1 (*C*–Ar), 149.7 (*C*–Ar), 149.8 (*C*-2), 152.4 (2 *C*–Ar); HRMS (ESI) calculated for $C_{35}H_{50}LiO_{10}Si$: 665.3329, $[M + Li]^+$ found 665.3355.

*6.1.3.2. (Z)-2,5-Anhydro-1-(2-naphtyl)-1-(3,4,5-trimethoxyphenyl)-1-deoxy-3,4:6,7-di-O-isopropylidene-D-gulo-hept-1-enitol (**8**).* Yield: 76% as a pale yellow solid; $R_f = 0.26$ (Hexane/EtOAc 7/3); $[\alpha]_D^{20} = -269^\circ$ (c = 0.37, $CHCl_3$); IR (film) ν 2986, 2938, 1645, 1580, 1505 cm^{-1}; ^1H NMR ($CDCl_3$, 400 MHz) δ 1.32 (s, 3H, C(CH_3)$_2$), 1.38 (s, 3H, C(CH_3)$_2$), 1.52 (s, 3H, C(CH_3)$_2$), 1.54 (s, 3H, C(CH_3)$_2$), 3.78 (s, 6H, 2 OCH_3), 3.84 (dd, 1H, *H*-7′, *J* = 8.5 Hz, *J* = 6.5 Hz), 3.91 (s, 3H, OCH_3), 4.15 (dd, 1H, *H*-5, *J* = 8.5 Hz, *J* = 5.0 Hz), 4.24 (dd, 1H, *H*-7, *J* = 8.5 Hz, *J* = 6.5 Hz), 4.50 (dt, 1H, *H*-6, *J* = 8.5 Hz, *J* = 6.5 Hz), 4.77 (dd, 1H, *H*-4, *J* = 6.0 Hz, *J* = 5.0 Hz), 5.04 (d, 1H, *H*-3, *J* = 6.0 Hz), 6.67 (s, 2H, *H*–Ar), 7.40–7.43 (m, 2H, *H*–Ar), 7.59 (dd, 1H, *H*–Ar, *J* = 8.5 Hz, *J* = 1.5 Hz), 7.70–7.82 (m, 4H, *H*–Ar); ^{13}C NMR ($CDCl_3$, 62.9 MHz) δ 25.2 (C(CH_3)$_2$), 25.3 (C(CH_3)$_2$), 26.2 (C(CH_3)$_2$), 27.0 (C(CH_3)$_2$), 56.0 (2 OCH_3), 60.9 (OCH_3), 66.0 (*C*-7), 75.7 (*C*-6), 78.4 (*C*-4), 80.4 (*C*-3), 85.1 (*C*-5), 108.2 (2 *C*–Ar), 109.8 (*C*(CH_3)$_2$), 112.6 (*C*(CH_3)$_2$), 120.7 (*C*-1), 125.6 (*C*–Ar), 125.7 (*C*–Ar), 127.1 (*C*–Ar), 127.4 (*C*–Ar), 127.9 (*C*–Ar), 128.2 (*C*–Ar), 128.8 (*C*–Ar), 132.4 (*C*–Ar), 133.3 (*C*–Ar), 134.8 (*C*–Ar), 136.2 (*C*–Ar), 137.0 (*C*–Ar), 151.1 (*C*-2), 152.6 (2 *C*–Ar); HRMS (ESI) calculated for $C_{32}H_{36}NaO_8$: 571.2302, $[M + Na]^+$ found 571.2306.

*6.1.3.3. (E)-2,5-Anhydro-1-(3-tertbutyldimethylsilyloxy-4-methoxyphenyl)-1-(3,4,5-trimethoxyphenyl)-1-deoxy-3,4:6,7-di-O-isopropyli-1-enitol (**11**).* Yield: 45% as a pale yellow solid; $R_f = 0.44$ (Hexane/EtOAc 7/3); $[\alpha]_D^{20} = -240^\circ$ (c = 0.48, $CHCl_3$); IR (film) ν 2987, 2938, 2857, 1654, 1578, 1511 cm^{-1}; ^1H NMR ($CDCl_3$, 400 MHz) δ 0.15 (s, 3H, Si(CH_3)$_2$), 0.16 (s, 3H, Si(CH_3)$_2$), 0.99 (s, 9H, SiC(CH_3)$_3$), 1.27 (s, 3H, C(CH_3)$_2$), 1.37 (s, 3H, C(CH_3)$_2$), 1.43 (s, 3H, C(CH_3)$_2$), 1.48 (s, 3H, C(CH_3)$_2$), 3.75 (s, 9H, 3 OCH_3), 3.78 (dd, 1H, *H*-7′, *J* = 8.5 Hz, *J* = 7.0 Hz), 3.83 (s, 3H, OCH_3), 4.04 (dd, 1H, *H*-5, *J* = 8.5 Hz, *J* = 4.5 Hz), 4.24 (dd, 1H, *H*-7, *J* = 8.5 Hz, *J* = 7.0 Hz), 4.50 (dt, 1H, *H*-6, *J* = 8.5 Hz, *J* = 7.0 Hz), 4.67 (dd, 1H, *H*-4, *J* = 6.0 Hz, *J* = 4.5 Hz), 4.95 (d, 1H, *H*-3, *J* = 6.0 Hz), 6.72 (s, 2H, *H*–Ar), 6.81 (d, 1H, *H*–Ar, *J* = 8.5 Hz), 6.85 (dd, 1H, *H*–Ar, *J* = 8.5 Hz, *J* = 2.0 Hz), 6.95 (d, 1H, *H*–Ar, *J* = 2.0 Hz); ^{13}C NMR ($CDCl_3$, 62.9 MHz) δ −4.7 (2 Si(CH_3)$_2$), 18.4 (Si*C*(CH_3)$_3$), 25.7 (C(CH_3)$_2$), 25.2 (C(CH_3)$_2$), 25.3 (SiC(CH_3)$_3$), 26.3 (C(CH_3)$_2$), 26.8 (C(CH_3)$_2$), 55.4 (OCH_3), 55.8 (2 OCH_3), 60.8 (OCH_3), 65.8 (*C*-7), 75.6 (*C*-6), 78.3 (*C*-4), 80.5 (*C*-3), 85.1 (*C*-5), 107.0 (2 *C*–Ar), 109.6 (*C*(CH_3)$_2$), 111.4 (*C*–Ar), 112.8 (*C*(CH_3)$_2$), 119.4 (*C*-1), 124.0 (*C*–Ar), 124.2 (*C*–Ar), 131.4 (*C*–Ar), 134.5 (*C*–Ar), 136.6 (*C*–Ar), 144.2 (*C*–Ar), 150.2 (*C*–Ar), 150.5 (*C*-2), 152.4 (2 *C*–Ar); HRMS (ESI) calculated for $C_{35}H_{50}NaO_{10}Si$: 681.3065, $[M + Na]^+$ found 681.3082.

*6.1.3.4. (Z)-2,5-Anhydro-1-(3-hydroxy-4-methoxyphenyl)-1-(3,4,5-trimethoxyphenyl)-1-deoxy-3,4:6,7-di-O-isopropylidene-D-gulo-hept-1-enitol (**6**).* The silyl ether **5** (0.14 mmol) was dissolved in dry CH_2Cl_2 (14 mL), tetrabutylammonium fluoride (156 μL, 0.16 mmol, 1.1 eq) was added slowly via syringe at 0 °C under argon. After 30 min, water (10 mL) was added. The organic layer was separated and the aqueous layer was extracted with CH_2Cl_2 (2 × 10 mL). Then the combined organic layers were washed with water (10 mL), dried ($MgSO_4$) and filtered. The filtrate was evaporated under reduced pressure and the residue was purified by chromatography (silica gel, Hexane/EtOAc). Yield: 70% as a pale yellow solid; $R_f = 0.19$ (Hexane/EtOAc 4/6); $[\alpha]_D^{20} = -276^\circ$ (c = 0.64, $CHCl_3$); IR (film) ν 3439 (OH), 2997, 2938 (C–H), 1656, 1580, 1508 cm^{-1}; ^1H NMR ($CDCl_3$, 400 MHz) δ 1.27 (s, 3H, C(CH_3)$_2$), 1.38 (s, 3H, C(CH_3)$_2$), 1.49 (s, 3H, C(CH_3)$_2$), 1.50 (s, 3H, C(CH_3)$_2$), 3.78 (s, 6H, 2 OCH_3), 3.79 (m, 1H, *H*-7′), 3.86 (s, 3H, OCH_3), 3.87 (s, 3H, OCH_3), 4.06 (dd, 1H, *H*-5, *J* = 8.0 Hz, *J* = 5.0 Hz), 4.23 (dd, 1H, *H*-7, *J* = 8.5 Hz, *J* = 6.5 Hz), 4.46 (dt, 1H, *H*-6, *J* = 8.0 Hz, *J* = 6.5 Hz), 4.69 (dd, 1H, *H*-4, *J* = 6.0 Hz, *J* = 5.0 Hz), 4.93 (d, 1H, *H*-3, *J* = 6.0 Hz), 5.64 (br s, 1H, O*H*), 6.59 (s, 2H, *H*–Ar), 6.78 (d, 1H, *H*–Ar, *J* = 8.5 Hz), 6.95 (dd, 1H, *H*–Ar, *J* = 8.5 Hz, *J* = 2.0 Hz), 6.99 (d, 1H, *H*–Ar, *J* = 2.0 Hz); ^{13}C NMR ($CDCl_3$, 62.9 MHz) δ 25.2 (C(CH_3)$_2$), 25.3 (C(CH_3)$_2$), 26.2 (C(CH_3)$_2$), 26.9 (C(CH_3)$_2$), 55.8 (OCH_3), 55.9 (2 OCH_3), 60.9 (OCH_3), 66.0 (*C*-7), 75.8 (*C*-6), 78.3 (*C*-4), 80.4 (*C*-3), 85.1 (*C*-5), 108.1 (2 *C*–Ar), 109.8 (*C*(CH_3)$_2$), 110.2 (*C*–Ar), 112.5 (*C*(CH_3)$_2$), 116.0 (*C*–Ar), 120.0 (*C*-1), 121.7 (*C*–Ar), 132.0 (*C*–Ar), 134.9 (*C*–Ar), 136.8 (*C*–Ar), 144.8 (*C*–Ar), 145.4 (*C*–Ar), 150.1 (*C*-2), 152.4 (2 *C*–Ar); HRMS (ESI) calculated for $C_{29}H_{36}NaO_{10}$: 567.2201, $[M + Na]^+$ found 567.2252.

*6.1.3.5. (E)-2,5-Anhydro-1-(3-hydroxy-4-methoxyhenyl)-1-(3,4,5-trimethoxyphenyl)-1-deoxy-3,4:6,7-di-O-isopropylidene-D-gulo-hept-1-enitol (**12**).* To a solution of silyl ether **11** (0.14 mmol) in dry CH_2Cl_2 (14 mL) was added slowly via syringe at 0 °C under argon tetrabutylammonium fluoride (1 M solution THF, 160 μL, 0.16 mmol, 1.1 eq). After 30 min, water (10 mL) was added. The organic layer was separated and the aqueous layer was extracted with CH_2Cl_2 (2 × 10 mL). The combined organic layers were washed with water (10 mL), dried ($MgSO_4$) and filtered. The filtrate was concentrated under reduced pressure and the residue was purified by chromatography (silica gel, Hexane/EtOAc). Yield: 55% as a pale yellow solid; $R_f = 0.27$ (Hexane/EtOAc 6/4); $[\alpha]_D^{20} = -247^\circ$ (c = 0.34, $CHCl_3$); IR (film) ν 2987, 2938, 2836, 1642, 1580, 1508 cm^{-1}; ^1H NMR ($CDCl_3$, 250 MHz) δ 1.29 (s, 3H, C(CH_3)$_2$), 1.37 (s, 3H, C(CH_3)$_2$), 1.43 (s, 3H, C(CH_3)$_2$), 1.50 (s, 3H, C(CH_3)$_2$), 3.76 (s, 6H, 2 OCH_3), 3.78 (m, 1H, *H*-7′), 3.84 (s, 3H, OCH_3), 3.92 (s, 3H, OCH_3), 4.04 (dd, 1H, *H*-5, *J* = 8.5 Hz, *J* = 4.5 Hz), 4.24 (dd, 1H, *H*-7, *J* = 8.5 Hz, *J* = 7.0 Hz), 4.50 (dt, 1H, *H*-6, *J* = 8.5 Hz, *J* = 7.0 Hz), 4.67 (dd, 1H, *H*-4, *J* = 6.0 Hz, *J* = 4.5 Hz), 4.99 (d, 1H, *H*-3, *J* = 6.0 Hz), 5.58 (br s, 1H, O*H*), 6.72 (s, 2H, *H*–Ar), 6.83 (d, 1H, *H*–Ar, *J* = 8.0 Hz), 6.87 (dd, 1H, *H*–Ar, *J* = 8.0 Hz, *J* = 2.0 Hz), 6.91 (d, 1H, *H*–Ar, *J* = 2.0 Hz); ^{13}C NMR ($CDCl_3$, 62.9 MHz) δ 25.2 (C(CH_3)$_2$), 25.4 (C(CH_3)$_2$), 26.4 (C(CH_3)$_2$), 26.8 (C(CH_3)$_2$), 55.8 (OCH_3), 55.9 (2 OCH_3), 60.8 (OCH_3), 65.8 (*C*-7), 75.7 (*C*-6), 78.3 (*C*-4), 80.5 (*C*-3), 85.0 (*C*-5), 107.1 (2 *C*–Ar), 109.7 (*C*(CH_3)$_2$), 110.0 (*C*–Ar), 112.8 (*C*(CH_3)$_2$), 117.0 (*C*–Ar), 119.5 (*C*-1), 122.9 (*C*–Ar), 132.0 (*C*–Ar), 134.4 (*C*–Ar), 136.8 (*C*–Ar), 144.9 (*C*–Ar), 145.7 (*C*–Ar), 150.5 (*C*-2), 152.4 (2 *C*–Ar); HRMS (ESI) calculated for $C_{29}H_{36}NaO_{10}$: 567.2201, $[M + Na]^+$ found 567.2250.

*6.1.3.6. (E)-2,5-Anhydro-1-(3-hydroxy-4-methoxyphenyl)-1-(3,4,5-trimethoxyphenyl)-1-deoxy-3,4-O-isopropylidene-D-gulo-hept-1-enitol (**19**).* To a stirred solution of the disubstituted *exo*-glycal **12** (0.34 mmol) in ethanol (2 mL) and water (2 mL) was added trifluoroacetic acid (2 mL), at 0 °C. After stirring 1 h at room temperature CH_2Cl_2 (60 mL) was added. The organic layer was washed with an aqueous solution of $NaHCO_3$ until pH = 7 and then with water (10 mL). The organic layer was dried over $MgSO_4$ and filtered. The solvent was removed under reduced pressure and the resulting product was purified by chromatography (silica gel, EtOAc). Yield: 62% as a pale yellow solid; $R_f = 0.44$ (EtOAc); $[\alpha]_D = -242^\circ$ (c = 0.25, $CHCl_3$); IR (Film) ν 3432, 2986, 2936, 2837, 1645, 1585, 1510 cm^{-1}; ^1H NMR ($CDCl_3$, 400 MHz) δ 1.33 (s, 3H, C(CH_3)$_2$), 1.52 (s, 3H, C(CH_3)$_2$), 2.20 (br s, 1H, OH), 2.95 (br s, 1H, OH), 3.76 (s, 6H, 2 OCH_3), 3.76–3.90 (m, 2H, *H*-7, *H*-7′), 3.84 (s, 3H, OCH_3), 3.92 (s, 3H, OCH_3), 4.10 (m, 1H, *H*-5), 4.19 (m, 1H, *H*-6), 4.79 (dd, 1H, *H*-4, *J* = 6.0 Hz, *J* = 4.0 Hz), 5.07 (d, 1H, *H*-3, *J* = 6.0 Hz), 5.61 (br s, 1H, O*H*), 6.59 (s, 2H, *H*–Ar), 6.83 (d, 1H, *H*–Ar, *J* = 8.0 Hz), 6.88 (dd, 1H, *H*–Ar, *J* = 8.0 Hz, *J* = 2.0 Hz), 6.91 (d, 1H, *H*–Ar, *J* = 2.0 Hz); ^{13}C NMR ($CDCl_3$, 100 MHz) δ 25.7 (C(CH_3)$_2$), 26.8 (C(CH_3)$_2$), 56.2 (OCH_3), 56.5 (2 OCH_3), 61.3 (OCH_3), 63.6 (*C*-7), 71.3 (*C*-6), 79.1 (*C*-4), 80.9 (*C*-3),

82.8 (*C*-5), 107.4 (2 *C*–Ar), 110.4 (*C*–Ar), 113.2 (*C*(CH_3)$_2$), 117.1 (*C*–Ar), 120.4 (*C*-1), 123.0 (*C*–Ar), 132.4 (*C*–Ar), 135.0 (*C*–Ar), 137.2 (*C*–Ar), 145.3 (*C*–Ar), 146.2 (*C*–Ar), 150.3 (*C*-2), 153.0 (2 *C*–Ar); HRMS (ESI) calculated for $C_{26}H_{32}NaO_{10}$ $[M + Na]^+$: 527.1888, found: 527.1897.

*6.1.3.7. 2-(1,1-Dibromomethylene)-1,3-diacetate-propan-1,3-diol (**22**).* To a stirred solution of CBr_4 (11.44 g, 34.5 mmol, 3 eq) in CH_2Cl_2 (60 mL) was added dropwise a solution of PPh_3 (18.10 g, 69 mmol, 6 eq) in CH_2Cl_2 (45 mL) at 0 °C, under argon and with exclusion of light (aluminium foil). Then a solution of **21** (2.0 g, 11.5 mmol) in CH_2Cl_2 (60 mL) was added dropwise. After stirring at room temperature for 2 h, hexane (800 mL) was added. The precipitate was removed by filtration and the filtrate was concentrated under reduced pressure. The residue was purified by column chromatography (silica gel, Hexane/EtOAc = 8/2). Yield: 85% as a white solid; $R_f = 0.57$ (Hexane/EtOAc 7/3); IR (film) ν 2959, 1744 cm^{-1}; ^1H NMR ($CDCl_3$, 250 MHz) δ 2.08 (s, 6H, OCOCH_3), 4.79 (s, 4H, CH_2); ^{13}C NMR ($CDCl_3$, 62.9 MHz) δ 20.6 (2 OCOCH_3), 63.9 (2 CH_2), 98.0 (*C*═C), 135.5 (C═*C*), 170.3 (2 OCOCH$_3$); HRMS (ESI) calculated for $C_8H_{10}Br_2NaO_4$: 352.8838, $[M + Na]^+$ found 352.8889.

*6.1.3.8. 2-(1-Bromo-1-(3,4,5-trimethoxyphenyl)methylene)-1,3-diacetate-propan-1,3-diol (**23**).* In a dry round-bottomed flask equipped with a condenser flushed with argon, 5 mL of dry DME, compound **22** (150 mg, 0.362 mmol), 3,4,5-trimethoxyphenylboronic acid (115 mg, 0.543 mmol, 1.5 eq), 2 M K_2CO_3 aqueous solution (3 eq) were stirred during 10 min, then tris(2-furyl)phosphine (26 mg, 0.109 mmol, 0.3 eq) and $PdCl_2(PPh_3)_2$ (13 mg, 0.018 mmol, 0.05 eq) were added as solids. The reaction mixture was stirred and heated at 85 °C for 24 h. The reaction was then allowed to cool to room temperature and was evaporated to dryness under reduced pressure. The residue was diluted with ethyl acetate (50 mL) and washed with NH_4Cl (2 × 5 mL). The solvent was removed under reduced pressure and the residue was purified by column chromatography (*n*-hexane/EtOAc). Yield: 35% as a pale yellow solid; $R_f = 0.58$ (Hexane/EtOAc 1/1); IR (film) ν 2991, 2938, 2830, 1741, 1647, 1577, 1502 cm^{-1}; ^1H NMR ($CDCl_3$, 250 MHz) 2.05 (s, 3H, OCOCH_3), 2.12 (s, 3H, OCOCH_3), 3.85 (s, 6H, OCH_3), 3.87 (s, 3H, OCH_3), 4.57 (s, 2H, CH_2), 4.97 (s, 2H, CH_2), 6.56 (s, 2H, *H*–Ar); ^{13}C NMR ($CDCl_3$, 62.9 MHz) δ 20.7 (2 OCOCH_3), 56.2 (OCH_3), 56.3 (OCH_3), 60.9 (OCH_3), 61.9 (CH_2), 65.1 (CH_2), 106.1 (2 *C*–Ar), 129.3 (*C*═C), 130.8 (*C*–Ar), 134.0 (C–Ar), 137.5 (*C*═C), 152.9 (2 *C*–Ar), 170.2 (OCOCH$_3$), 170.6 (OCOCH$_3$); HRMS (ESI) calculated for $C_{17}H_{21}BrNaO_7$: 439.0363, $[M + Na]^+$ found 441.0350.

*6.1.3.9. 2-(1-(3-Tert-butyldimethylsilyloxy-4-methoxyphenyl)-1-(3,4,5-trimethoxyphenyl)methylene)-1,3-diacetate-propan-1,3-diol (**25**).* In a dry round-bottomed flask equipped with a condenser flushed with argon, 5 mL of dry DME, compound **23** (151 mg, 0.362 mmol, 1 eq), boronic acid (2 eq), 2 M K_2CO_3 aqueous solution (4 eq) were stirred during 10 min. $Pd(PPh_3)_4$ (20 mg, 0.018 mmol, 0.05 eq) was added as solids. The reaction mixture was stirred and heated at 85 °C during 24 h. The reaction was then allowed to cool to room temperature and was evaporated to dryness under reduced pressure. The residue was diluted with ethyl acetate (50 mL) and washed with NH_4Cl (2 × 5 mL). The dried organic layer was concentrated under reduced pressure and the residue was purified by chromatography (*n*-hexane/EtOAc). Yield: 53% as a pale yellow solid; $R_f = 0.62$ (Hexane/EtOAc 1/1); IR (film) ν 2954, 2933, 2857, 1742, 1642, 1580, 1508 cm^{-1}; ^1H NMR ($CDCl_3$, 400 MHz) δ 0.11 (s, 6H, Si(CH_3)$_2$), 0.96 (s, 9H, SiC(CH_3)$_3$), 2.08 (s, 3H, OCOCH_3), 2.09 (s, 3H, OCOCH_3), 3.77 (s, 6H, OCH_3), 3.81 (s, 3H, OCH_3), 3.85 (s, 3H, OCH_3), 4.68 (s, 2H, CH_2), 4.70 (s, 2H, CH_2), 6.36 (s, 2H, *H*–Ar), 6.69 (s, 1H, *H*–Ar), 6.70 (m, 1H, *H*–Ar), 6.79 (m, 1H, *H*–Ar); ^{13}C NMR ($CDCl_3$, 62.9 MHz) δ −4.7 (2 Si(CH_3)$_2$), 18.4 (OCOCH$_3$), 20.9 (OCOCH_3), 21.0 (SiC(CH_3)$_3$), 25.6 (3 SiC(CH_3)$_3$), 55.4 (OCH_3), 56.0 (2 OCH_3), 60.9 (OCH_3), 63.3 (CH_2), 63.4 (CH_2), 106.7 (2 *C*–Ar), 111.5 (*C*–Ar), 122.2 (*C*–Ar), 123.0 (*C*–Ar), 126.0 (*C*═C), 132.7 (*C*–Ar), 136.2 (*C*–Ar), 137.7 (*C*–Ar), 144.4 (*C*–Ar), 149.0 (*C*═C), 150.9 (*C*–Ar), 152.8 (2 *C*–Ar), 170.7 (OCOCH$_3$), 170.8 (OCOCH$_3$); HRMS (ESI) calculated for $C_{30}H_{42}NaO_9Si$: 597.2490, $[M + H]^+$ found 597.2492.

*6.1.3.10. 2-(1-(3-Hydroxy-4-methoxyphenyl)-1-(3,4,5-trimethoxyphenyl)methylene)-1,3-diacetate-propan-1,3-diol (**26**).* To a solution of silyl ether **25** (0.14 mmol) in dry CH_2Cl_2 (14 mL) was added slowly via syringe at 0 °C under argon tetrabutylammonium fluoride (1 M solution in THF, 160 μL, 0.16 mmol, 1.1 eq) After 30 min, water (10 mL) was added. The organic layer was separated and the aqueous layer was extracted with CH_2Cl_2 (2 × 10 mL). Then the combined organic layers were washed with water (10 mL), dried ($MgSO_4$) and filtered. The solvent was evaporated under reduced pressure and the residue was purified by chromatography (silica gel, Hexane/EtOAc). Yield: 90% as a pale yellow solid; $R_f = 0.25$ (Hexane/EtOAc 1/1); IR (film) ν 3418, 2997, 2943, 2836, 1736, 1650, 1580, 1508 cm^{-1}; ^1H NMR ($CDCl_3$, 250 MHz) δ 2.07 (s, 3H, OCOCH_3), 2.09 (s, 3H, OCOCH_3), 3.78 (s, 6H, OCH_3), 3.84 (s, 3H, OCH_3), 3.88 (s, 3H, OCH_3), 4.67 (s, 2H, CH_2), 4.68 (s, 2H, CH_2), 5.65 (br s, 1H, O*H*), 6.36 (s, 2H, *H*–Ar), 6.67 (dd, 1H, *H*–Ar, $J = 8.0$ Hz, $J = 2.0$ Hz), 6.72 (d, 1H, *H*–Ar, $J = 2.0$ Hz), 6.79 (d, 1H, *H*–Ar, $J = 8.0$ Hz); ^{13}C NMR ($CDCl_3$, 62.9 MHz) δ 20.9 (OCOCH_3), 21.0 (OCOCH_3), 55.9 (OCH_3), 56.1 (2 OCH_3), 60.8 (OCH_3), 63.1 (CH_2), 63.2 (CH_2), 106.6 (2 *C*–Ar), 110.1 (*C*–Ar), 115.6 (*C*–Ar), 121.1 (*C*–Ar), 126.5 (*C*═C), 133.3 (*C*–Ar), 136.0 (*C*–Ar), 137.7 (*C*–Ar), 145.2 (*C*–Ar), 146.4 (*C*–Ar), 148.8 (*C*═C), 152.8 (2 *C*–Ar), 170.7 (OCOCH$_3$), 170.8 (OCOCH$_3$); HRMS (ESI) calculated for $C_{24}H_{28}NaO_9$ $[M + H]^+$: 483.1626, found: 483.1625.

*6.1.3.11. 2-(1-(2-Naphtyl)-1-(3,4,5-trimethoxyphenyl)methylene)-propan-1,3-diol (**32**).* To a solution of **28** (0.24 mmol) in methanol (5 mL) was added at 0 °C under argon a freshly prepared solution of sodium methanolate in methanol (1 mL). After 30 min, Amberlite IR-120 (H^+) was added until pH = 7. After filtration, the solvent was removed under reduced pressure and the residue was purified by chromatography (Hexane/EtOAc). Yield: 83% as a pale yellow solid; $R_f = 0.20$ (Hexane/EtOAc 1/2); IR (film) ν 3402, 3051, 2933, 2851, 1650, 1580 (OMe), 1503 cm^{-1}; ^1H NMR ($CDCl_3$, 400 MHz) δ 3.77 (s, 6H, OCH_3), 3.86 (s, 3H, OCH_3), 4.45 (br s, 4H, CH_2), 6.46 (s, 2H, *H*–Ar), 7.46–7.52 (m, 3H, *H*–Ar), 7.70 (m, 1H, *H*–Ar), 7.75–7.85 (m, 3H, *H*–Ar); ^{13}C NMR ($CDCl_3$, 62.9 MHz) δ 56.1 (2 OCH_3), 60.9 (OCH_3), 63.7 (CH_2), 63.8 (CH_2), 107.1 (2 *C*–Ar), 126.2 (*C*–Ar), 126.3 (*C*–Ar), 127.5 (*C*–Ar), 127.6 (*C*–Ar), 127.7 (*C*–Ar), 128.1 (*C*–Ar), 128.3 (*C*–Ar), 132.6 (*C*–Ar), 132.9 (*C*–Ar), 135.3 (*C*═C), 136.3 (*C*–Ar), 137.4 (*C*–Ar), 138.0 (*C*–Ar), 143.5 (*C*═C), 152.8 (2 *C*–Ar); HRMS (ESI) calculated for $C_{23}H_{24}NaO_5$: 403.1516, $[M + H]^+$ found: 403.1497.

6.2. Antiproliferative assays (NCI60 cell lines panel)

The human tumor cell lines of the cancer screening panel are grown in RPMI 1640 medium containing 5% fetal bovine serum and 2 mM L-glutamine. For a typical screening experiment, cells are inoculated into 96-well microtiter plates in 100 μL at plating densities ranging from 5000 to 40,000 cells/well depending on the doubling time of individual cell lines. After cell inoculation, the microtiter plates are incubated at 37 °C, 5% CO_2, 95% air and 100% relative humidity for 24 h prior to addition of experimental drugs. After 24 h, two plates of each cell line are fixed *in situ* with TCA, to represent a measurement of the cell population for each cell line at the time of drug addition (Tz). Experimental drugs are solubilised in dimethyl sulfoxide at 400-fold the desired final maximum test concentration and stored frozen prior to use. At

the time of drug addition, an aliquot of frozen concentrate is thawed and diluted to twice the desired final maximum test concentration with complete medium containing 50 μg/mL gentamicin. Additional four, 10-fold or 1/2 log serial dilutions are made to provide a total of five drug concentrations plus control. Aliquots of 100 μL of these different drug dilutions are added to the appropriate microtiter wells already containing 100 μL of medium, resulting in the required final drug concentrations. Following drug addition, the plates are incubated for an additional 48 h at 37 °C, 5% CO_2, 95% air, and 100% relative humidity. For adherent cells, the assay is terminated by the addition of cold TCA. Cells are fixed *in situ* by the gentle addition of 50 μL of cold 50% (w/v) TCA (final concentration, 10% TCA) and incubated for 60 min at 4 °C. The supernatant is discarded, and the plates are washed five times with tap water and air dried. Sulforhodamine B (SRB) solution (100 μL) at 0.4% (w/v) in 1% acetic acid is added to each well, and plates are incubated for 10 min at room temperature. After staining, unbound dye is removed by washing five times with 1% acetic acid and the plates are air dried. Bound stain is subsequently solubilised with 10 mM trizma base, and the absorbance is read on an automated plate reader at a wavelength of 515 nm. For suspension cells, the methodology is the same except that the assay is terminated by fixing settled cells at the bottom of the wells by gently adding 50 μL of 80% TCA (final concentration, 16% TCA). Three dose response parameters (GI_{50}, TGI and LC_{50}) were calculated for each experimental agent and each cell line [38].

6.3. Antiproliferative assays (ICSN 9 cell lines panel)

The human cell lines were obtained from ATCC, except when otherwise stated: HCT15 (colon adenocarcinoma), SK-OV3 (ovary adenocarcinoma from NCI), OVCAR8 (ovary adenocarcinoma from Dr Liscovitch, Rehovot, Israel), SF268 (glioblastoma from NCI), PC-3 (prostate adenocarcinoma), HL60 (promyeocytic leukemia), K562 (chronic myelogenous leukemia) and MDA-MB-231 (breast adenocarcinoma) were grown in RPMI medium supplemented with 10% fetal calf serum, in the presence of penicillin, streptomycin and fungizone in 75 cm^2 flask under 5% CO_2. HL60R/R10 was originated from Oncodesign and maintained in complete RPMI medium containing 100 nM adriamycin.

Cells were plated in 96-well tissue culture plates in 200 μL medium and treated 24 h later with 2 μL stock solution of compounds dissolved in DMSO using a Biomek 3000 (Beckman–Coulter). Controls received the same volume of DMSO (1% final volume). After 72 h exposure, MTS reagent (Promega) was added and incubated for 3 h at 37 °C: the absorbance was monitored at 490 nm and results expressed as the inhibition of cell proliferation calculated as the ratio [(1 − (OD490 treated/OD490 control)) × 100] in triplicate experiments. For IC_{50} determination [50% inhibition of cell proliferation], cells were incubated for 72 h following the same protocol with compound concentrations ranged 5 nM to 100 μM in separate duplicate experiments.

6.4. Inhibition of tubulin assembly

Sheep brain microtubule proteins were purified by two cycles of assembly/disassembly at 37 °C/0 °C and then dissolved in MES buffer: 100 mM MES (2-[*N*-morpholino]-ethanesulfonic acid, pH 6.6), 1 mM EGTA (ethyleneglycol-bis[ß-aminoethyl ether]-*N*,*N*,*N*′,*N*′-tetraacetic acid), 0.5 mM $MgCl_2$. All samples were dissolved in DMSO, incubated at 37 °C for 10 min and at 0 °C for 5 min before evaluation of the tubulin assembly rate. The tubulin assembly assay was realized according to a slightly modified Guénard protocol using deoxypodophyllotoxin as reference compound [47].

6.5. Computational procedure

All molecular modelling studies were performed with Schrodinger Molecular Modelling Suite 2010 [48]. Maestro is the interface piloting the diverse modules. Macromodel was used to prepare ligands and Glide is the docking software. Calculations were run on a Linux station: Intel® Core™ i7 CPU 950 @ 3.07 GHz. Tubulin complex with DAMA-colchicine was retrieved from the protein data bank [40]. Subunits C, D and E were removed. Only subunits A, B (colchicine binding site) and small molecules DAMA-colchicine (CN2), GTP and Mg^{2+} ion in this site were conserved. Structures were next prepared using the workflow Protein Preparation Wizard. Structures were preprocessed (hydrogen atoms added, incomplete residues filled …), bond orders and connections of ligands were manually corrected. An exhaustive sampling was done regarding hydrogen bond assignment and the complex was finally refined by a minimization stage with a constraint to converge to a structure with an RMSD of 0.3 Å (OPLS2005 force field), essentially in order to remove steric clashes. Docking calculations were performed with standard precision. Ligand flexibility is taken into account and the option of sampling of ring conformation was activated. CA-4 was built within the builder module of Maestro [40] and was submitted to Corina a 3D structure generator [49,50]. This conformation was next minimized within Macromodel using the OPLS 2005 force field [42]. Next the optimized energy minimized conformations have been submitted to the docking software Glide [40]. Ten poses at most were written out per ligand and a post-docking minimization stage was performed with 1000 poses per ligand to be included.

Acknowledgments

We thank F. Dupire, B. Fernette and P. Lemière for technical assistance.

Appendix. Supplementary data

Experimental procedures and spectroscopic data for intermediate and final compounds, additional cytotoxicity data in the NCI60 cell lines and in the ciblothèque-ICSN cell lines.

Supplementary data associated with this article can be found in the online version, at doi:10.1016/j.ejmech.2011.05.021.

References

[1] M. Saleem, H.J. Kim, M.S. Ali, Y.S. Lee, An update on bioactive plant lignans, Nat. Prod. Rep. 22 (2005) 696–716.
[2] C.M. Lin, S.B. Singh, P.S. Chu, R.O. Dempcy, J.M. Schmidt, G.R. Pettit, E. Hamel, Interactions of tubulin with potent natural and synthetic analogs of the antimitotic agent combretastatin: a structure–activity study, Mol. Pharmacol. 34 (1988) 200–208.
[3] G.R. Pettit, S.B. Singh, M.R. Boyd, E. Hamel, R.K. Pettit, J.M. Schmidt, F. Hogan, Antineoplastic agents. 291. Isolation and synthesis of combretastatins A-4, A-5, and A-6(1a), J. Med. Chem. 38 (1995) 1666–1672.
[4] G.R. Pettit, M.P. Grealish, D.L. Herald, M.R. Boyd, E. Hamel, R.K. Pettit, Antineoplastic agents. 443. Synthesis of the cancer cell growth inhibitor hydroxyphenstatin and its sodium diphosphate prodrug, J. Med. Chem. 43 (2000) 2731–2737.
[5] C.M. Lin, H.H. Ho, G.R. Pettit, E. Hamel, Antimitotic natural products combretastatin A-4 and combretastatin A-2: studies on the mechanism of their inhibition of the binding of colchicine to tubulin, Biochemistry 28 (1989) 6984–6991.
[6] P. Hinnen, F.A.L.M. Eskens, Vascular disrupting agents in clinical development, Br. J. Cancer 96 (2007) 1159–1165.
[7] D.J. Chaplin, G.R. Pettit, S.A. Hill, Anti-vascular approaches to solid tumor therapy: evaluation of combretastatin A4 phosphate, Anticancer Res. 19 (1999) 189–196.
[8] C.J. Mooney, G. Nagaiah, P. Fu, J.K. Wasman, M.M. Cooney, P.S. Savvides, J.A. Bokar, A. Dowlati, D. Wang, S.S. Agarwala, S.M. Flick, P.H. Hartman, J.D. Ortiz, P. Lavertu, S.C. Remick, A phase II trial of fosbretabulin in advanced anaplastic thyroid carcinoma and correlation of baseline serum-soluble intracellular adhesion molecule-1 with outcome, Thyroid 19 (2009) 233–240.

[9] G.C. Tron, T. Pirali, G. Sorba, F. Pagliai, S. Busacca, A.A. Genazzani, Medicinal chemistry of combretastatin A4: present and future directions, J. Med. Chem. 49 (2006) 3033–3044.
[10] J.-P. Liou, J.-Y. Chang, C.-W. Chang, C.-Y. Chang, N. Mahindroo, F.-M. Kuo, H.-P. Hsieh, Synthesis and structure–activity relationships of 3-amino-benzophenones as antimitotic agents, J. Med. Chem. 47 (2004) 2897–2905.
[11] M.G. Banwell, E. Hamel, D.C.R. Hockless, P. Verdier-Pinard, A.C. Willis, D.J. Wong, 4,5-Diaryl-1*H*-pyrrole-2-carboxylates as combretastatin A-4/lamellarin T hybrids: synthesis and evaluation as anti-mitotic and cytotoxic agents, Bioorg. Med. Chem. 14 (2006) 4627–4638.
[12] E.G. Barbosa, L.A.S. Bega, A. Beatriz, T. Sarkar, E. Hamel, M.S. do Amaral, D. Pires de Lima, A diaryl sulfide, sulfoxide, and sulfone bearing structural similarities to combretastatin A-4, Eur. J. Med. Chem. 44 (2009) 2685–2688.
[13] (a) R. Romagnoli, P.G. Baraldi, M.D. Carrion, O. Cruz-Lopez, C. Lopez Cara, G. Basso, G. Viola, M. Khedr, J. Balzarini, S. Mahboobi, A. Sellmer, A. Brancale, E. Hamel, 2-Arylamino-4-amino-5-aroylthiazoles. One-pot synthesis and biological evaluation of a new class of inhibitors of tubulin polymerization, J. Med. Chem. 52 (2009) 5551–5555;
(b) R. Romagnoli, P.G. Baraldi, O. Cruz-Lopez, C. Lopez Cara, M.D. Carrion, A. Brancale, E. Hamel, L. Chen, R. Bortolozzi, G. Basso, G. Viola, Synthesis and antitumor activity of 1,5-disubstituted 1,2,4-triazoles as cis-restricted combretastatin analogues, J. Med. Chem. 53 (2010) 4248–4258.
[14] B. Burja, T. Cimbora-Zovko, S. Tomic, T. Jelusic, M. Kocevar, S. Polanc, M. Osmak, Pyrazolone-fused combretastatins and their precursors: synthesis, cytotoxicity, antitubulin activity and molecular modeling studies, Bioorg. Med. Chem. 18 (2010) 2375–2387.
[15] (a) K. Odlo, J. Fournier-Dit-Chabert, S. Ducki, O.A.B.S.M. Gani, I. Sylte, T.V. Hansen, 1,2,3-Triazole analogs of combretastatin A-4 as potential microtubule-binding agents, Bioorg. Med. Chem. 18 (2010) 6874–6885;
(b) C. Bailly, C. Bal, P. Barbier, S. Combes, J.-P. Finet, M.-P. Hildebrand, V. Peyrot, N. Wattez, Synthesis and biological evaluation of 4-arylcoumarin analogues of combretastatins, J. Med. Chem. 46 (2003) 5437–5444.
[16] N. Ty, J. Kaffy, A. Arrault, S. Thoret, R. Pontikis, J. Dubois, L. Morin-Allory, J.-C. Florent, Synthesis and biological evaluation of *cis*-locked vinylogous combretastatin-A4 analogues: derivatives with a cyclopropyl-vinyl or a cyclopropyl-amide bridge, Bioorg. Med. Chem. Lett. 19 (2009) 1318–1322.
[17] A.B.S. Maya, C. Perez-Melero, C. Mateo, D. Alonso, J.L. Fernandez, C. Gajate, F. Mollinedo, R. Pelaez, E. Caballero, M. Medarde, Further naphthylcombretastatins. An investigation on the role of the naphthalene moiety, J. Med. Chem. 48 (2005) 556–568.
[18] A.B. Sanchez Maya, C. Perez-Melero, N. Salvador, R. Pelaez, E. Caballero, M. Medarde, New naphthylcombretastatins. Modifications on the ethylene bridge, Bioorg. Med. Chem. 13 (2005) 2097–2107.
[19] G.R. Pettit, B. Toki, D.L. Herald, P. Verdier-Pinard, M.R. Boyd, E. Hamel, R.K. Pettit, Antineoplastic agents. 379. Synthesis of phenstatin phosphate, J. Med. Chem. 41 (1998) 1688–1695.
[20] C. Alvarez, R. Alvarez, P. Corchete, C. Perez-Melero, R. Pelaez, M. Medarde, Exploring the effect of 2,3,4-trimethoxyphenyl moiety as a component of indolephenstatins, Eur. J. Med. Chem. 45 (2010) 588–597.
[21] G.R. Pettit, M.P. Grealish, M.K. Jung, E. Hamel, R.K. Pettit, J.C. Chapuis, J.M. Schmidt, Antineoplastic agents. 465. Structural modification of resveratrol: sodium resverastatin phosphate, J. Med. Chem. 45 (2002) 2534–2542.
[22] (a) R. Romagnoli, P.G. Baraldi, M.K. Jung, M.A. Iaconinoto, M.D. Carrion, V. Remusat, D. Preti, M.A. Tabrizi, F. Francesca, E. De Clercq, J. Balzarini, E. Hamel, Synthesis and preliminary biological evaluation of new anti-tubulin agents containing different benzoheterocycles, Bioorg. Med. Chem. Lett. 15 (2005) 4048–4052;
(b) R. Romagnoli, P.G. Baraldi, M.G. Pavani, M.A. Tabrizi, D. Preti, F. Fruttarolo, L. Piccagli, M.K. Jung, E. Hamel, M. Borgatti, R. Gambari, Synthesis and biological evaluation of 2-amino-3-(3′,4′,5′-trimethoxybenzoyl)-5-aryl thiophenes as a new class of potent antitubulin agents, J. Med. Chem. 49 (2006) 3906–3915;
(c) R. Romagnoli, P.G. Baraldi, V. Remusat, M.D. Carrion, C.L. Cara, D. Preti, F. Fruttarolo, M.G. Pavani, M.A. Tabrizi, M. Tolomeo, S. Grimaudo, J. Balzarini, M.A. Jordan, E. Hamel, Synthesis and biological evaluation of 2-(3′,4′,5′-trimethoxybenzoyl)-3-amino 5-aryl thiophenes as a new class of tubulin inhibitors, J. Med. Chem. 49 (2006) 6425–6428.
[23] (a) C. Alvarez, R. Alvarez, P. Corchete, C. Perez-Melero, R. Pelaez, M. Medarde, Synthesis and biological activity of naphthalene analogues of phenstatins: naphthylphenstatins, Bioorg. Med. Chem. Lett. 17 (2007) 3417–3420;
(b) C. Alvarez, R. Alvarez, P. Corchete, C. Perez-Melero, R. Pelaez, M. Medarde, Naphthylphenstatins as tubulin ligands: synthesis and biological evaluation, Bioorg. Med. Chem. 16 (2008) 8999–9008.
[24] S. Jiang, C. Crogan-Grundy, J. Drewe, B. Tseng, S.X. Cai, Discovery of (naphthalen-4-yl)(phenyl)methanones and *N*-methyl-*N*-phenylnaphthalen-1-amines as new apoptosis inducers using a cell- and caspase-based HTS assay, Bioorg. Med. Chem. Lett. 18 (2008) 5725–5728.
[25] S. Ducki, G. MacKenzie, B. Greedy, S. Armitage, J. Fournier Dit Chabert, E. Bennett, J. Nettles, J.P. Snyder, N.J. Lawrence, Combretastatin-like chalcones as inhibitors of microtubule polymerisation. Part 2: structure-based discovery of alpha-aryl chalcones, Bioorg. Med. Chem. 17 (2009) 7711–7722.
[26] R. Romagnoli, P.G. Baraldi, M.D. Carrion, O. Cruz-Lopez, M. Tolomeo, S. Grimaudo, A. Di Cristina, M.R. Pipitone, J. Balzarini, A. Brancale, E. Hamel, Substituted 2-(3′,4′,5′-trimethoxybenzoyl)-benzo[b]thiophene derivatives as potent tubulin polymerization inhibitors, Bioorg. Med. Chem. 18 (2010) 5114–5122.
[27] J.-P. Liou, Y.-L. Chang, F.-M. Kuo, C.-W. Chang, H.-Y. Tseng, C.-C. Wang, Y.-N. Yang, J.-Y. Chang, S.-J. Lee, H.-P. Hsieh, Concise synthesis and structure–activity relationships of combretastatin A-4 analogues, 1-aroylindoles and 3-aroylindoles, as novel classes of potent antitubulin agents, J. Med. Chem. 47 (2004) 4247–4257.
[28] G. Dupeyre, G.G. Chabot, S. Thoret, X. Cachet, J. Seguin, D. Guenard, F. Tillequin, D. Scherman, M. Koch, S. Michel, Synthesis and biological evaluation of (3,4,5-trimethoxyphenyl)indol-3-ylmethane derivatives as potential antivascular agents, Bioorg. Med. Chem. 14 (2006) 4410–4426.
[29] J.-P. Liou, N. Mahindroo, C.-W. Chang, F.-M. Guo, S.W.-H. Lee, U.-K. Tan, T.-K. Yeh, C.-C. Kuo, Y.-W. Chang, P.-H. Lu, Y.-S. Tung, K.-T. Lin, J.-Y. Chang, H.-P. Hsieh, Structure–activity relationship studies of 3-aroylindoles as potent antimitotic agents, ChemMedChem 1 (2006) 1106–1118.
[30] Y. Jin, Z.Y. Zhou, W. Tian, Q. Yu, Q.Y. Longa, 4′-Alkoxyl substitution enhancing the anti-mitotic effect of 5-(3′,4′,5′-substituted)anilino-4-hydroxy-8-nitroquinazolines as a novel class of anti-microtubule agents, Bioorg. Med. Chem. Lett. 16 (2006) 5864–5869.
[31] C. Alvarez, R. Alvarez, P. Corchete, J.L. Lopez, C. Perez-Melero, R. Pelaez, M. Medarde, Diarylmethyloxime and hydrazone derivatives with 5-indolyl moieties as potent inhibitors of tubulin polymerization, Bioorg. Med. Chem. 16 (2008) 5952–5961.
[32] S. Messaoudi, B. Treguier, A. Hamze, O. Provot, J.-F. Peyrat, J.R. De Losada, J.-M. Liu, J. Bignon, J. Wdzieczak-Bakala, S. Thoret, J. Dubois, J.-D. Brion, M. Alami, Isocombretastatins A versus combretastatins A: the forgotten isoCA-4 isomer as a highly promising cytotoxic and antitubulin agent, J. Med. Chem. 52 (2009) 4538–4542.
[33] R. Alvarez, C. Alvarez, F. Mollinedo, B.G. Sierra, M. Medarde, R. Pelaez, Isocombretastatins A: 1,1-diarylethenes as potent inhibitors of tubulin polymerization and cytotoxic compounds, Bioorg. Med. Chem. 17 (2009) 6422–6431.
[34] A. Novoa, N. Pellegrini-Moïse, S. Lamandé-Langle, Y. Chapleur, Efficient access to disubstituted exo-glycals. Application to the preparation of C-glycosyl compounds, Tetrahedron Lett. 50 (2009) 6484–6487.
[35] S.K. Chattopadhyay, T.R.S. Kumar, P.R. Maulik, S. Srivastava, A. Garg, A. Sharon, A.S. Negi, S.P.S. Khanuja, Absolute configuration and anticancer activity of taxiresinol and related lignans of *Taxus wallichiana*, Bioorg. Med. Chem. 11 (2003) 4945–4948.
[36] (a) C. Taillefumier, Y. Chapleur, Synthesis and uses of exo-glycals, Chem. Rev. 104 (2004) 263–292;
(b) Y. Lakhrissi, C. Taillefumier, F. Chrétien, Y. Chapleur, Facile dibromoolefination of lactones using bromomethylene triphenylphosphorane, Tetrahedron Lett. 42 (2001) 7265–7268.
[37] (a) K.S. Feldman, Cyclization pathways of a (*Z*)-stilbene-derived bis(ortho quinone monoketal), J. Org. Chem. 62 (1997) 4983–4990;
(b) C.A. Ocasio, T.S. Scanlan, Characterization of thyroid hormone receptor alpha (TRα)-specific analogs with varying inner- and outer-ring substituents, Bioorg. Med. Chem. 16 (2008) 762–770.
[38] National Cancer Institute (NCI), Bethesda. Available from: http://dtp.nci.nih.gov.
[39] R.B.G. Ravelli, B. Gigant, P.A. Curmi, I. Jourdain, S. Lachkar, A. Sobel, M. Knossow, Insight into tubulin regulation from a complex with colchicine and a stathmin-like domain, Nature (London, U.K 428 (2004) 198–202.
[40] 3D structure of phenstatin and phenstatin-like compounds were next built from the best CA-4 docked pose and then optimized again by minimization. Available from: http://www.rcsb.org/pdb/home/home.do.
[41] R. Bai, K.D. Paull, C.L. Herald, L. Malspeis, G.R. Pettit, E. Hamel, Halichondrin B and homohalichondrin B, marine natural products binding in the vinca domain of tubulin. Discovery of tubulin-based mechanism of action by analysis of differential cytotoxicity data, J. Biol. Chem. 266 (1991) 15882–15889.
[42] K.D. Paull, C.M. Lin, L. Malspeis, E. Hamel, Identification of novel antimitotic agents acting at the tubulin level by computer-assisted evaluation of differential cytotoxicity data, Cancer Res. 52 (1992) 3892–3900.
[43] F. Bellina, S. Cauteruccio, S. Montib, R. Rossia, Novel imidazole-based combretastatin A-4 analogues: evaluation of their in vitro antitumor activity and molecular modeling study of their binding to the colchicine site of tubulin, Bioorg. Med. Chem. Lett. 16 (2006) 5757–5762.
[44] A. Minocha, B.H. Long, Inhibition of the DNA catenation activity of type II topoisomerase by VP16-213 and VM26, Biochem. Biophys. Res. Commun. 122 (1984) 165–170.
[45] P. Meresse, E. Dechaux, C. Monneret, E. Bertounesque, Etoposide: discovery and medicinal chemistry, Curr. Med. Chem. 11 (2004) 2443–2466.
[46] H. Xu, M. Lv, X. Tian, Review on hemisynthesis, biosynthesis, biological activities, mode of action, and structure-activity relationship of podophyllotoxins: 2003–2007, Curr. Med. Chem. 16 (2009) 327–349.
[47] F. Zavala, D. Guenard, J.-P. Robin, E. Brown, Structure–antitubulin activity relationships in steganacin congeners and analogues. Inhibition of tubulin polymerization in vitro by isodeoxypodophyllotoxin, J. Med. Chem. 23 (1980) 546–549.
[48] Maestro, version 9.1, Glide, version 5.6, MacroModel, version 9.8, Schrödinger, LLC, New York, NY, 2010.
[49] Available from: http://www.molecular-networks.com/products/corina.
[50] J. Sadowski, J. Gasteiger, From atoms and bonds to three-dimensional atomic coordinates: automatic model builders, Chem. Rev. 93 (1993) 2567–2581.